OncoImmunology 3, e28989; June 2014; © 2014 Landes Bioscience

Stromal niche communalities underscore the contribution of the matricellular protein SPARC to B-cell development and lymphoid malignancies

Sabina Sangaletti[1,†], Claudio Tripodo[2,†], Paola Portararo[1], Matteo Dugo[3], Caterina Vitali[1], Laura Botti[1], Carla Guarnotta[2], Barbara Cappetti[1], Alessandro Gulino[2], Ilaria Torselli[1], Patrizia Casalini[4], Claudia Chiodoni[1], and Mario P Colombo[1,*]

[1]Molecular Immunology Unit; Department of Experimental Oncology and Molecular Medicine; Fondazione IRCCS Istituto Nazionale Tumori; Milan, Italy; [2]Tumor Immunology Unit, Department of Health Sciences; University of Palermo; Palermo, Italy; [3]Functional Genomics Core Facility; Department of Experimental Oncology and Molecular Medicine; Fondazione IRCCS Istituto Nazionale Tumori; Milan, Italy; [4]Molecular Therapies Unit; Department of Experimental Oncology and Molecular Medicine; Fondazione IRCCS Istituto Nazionale Tumori; Milan, Italy

[†]These authors contributed equally to this work.

Keywords: B cell development, SPARC, bone marrow niches, lymphomas, microenvironment

Abbreviations: BCR, B-cell receptor; BM, bone marrow; BMT, bone marrow transplantation; CLL, chronic lymphocytic leukemia; DLBCL, diffuse large B-cell lymphoma; DLL-1, delta-like protein 1; ECM, extracellular matrix; FDC, follicular dendritic cells; FL, follicular lymphoma; FoB, follicular B-cell; GC, germinal center; GE, gene expression; HSC, hematopoietic stem cells; KO, knock out; LAIR-1, leukocyte-associated immunoglobulin-like receptor 1; MSC, mesenchymal stromal cells; MZB, marginal zone B; MZL, marginal zone lymphoma; NHL, non-Hodgkin lymphoma; SLO, secondary lymphoid organs: SPARC, secreted protein acidic and rich in cysteine

Neoplastic B-cell clones commonly arise within secondary lymphoid organs (SLO). However, during disease progression, lymphomatous cells may also colonize the bone marrow (BM), where they localize within specialized stromal niches, namely the osteoblastic and the vascular niche, according to their germinal center- or extra-follicular-derivation, respectively. We hypothesized the existence of common stromal motifs in BM and SLO B-cell lymphoid niches involved in licensing normal B-cell development as well as in fostering transformed B lymphoid cells. Thus, we tested the expression of prototypical mesenchymal stromal cell (MSC) markers and regulatory matricellular proteins in human BM and SLO under physiologically unperturbed conditions and during B-cell lymphoma occurrence. We identified common stromal features in the BM osteoblastic niche and SLO germinal center (GC) microenvironments, traits that were also enriched within BM infiltrates of GC-associated B-cell lymphomas, suggesting that stromal programs involved in central and peripheral B-cell lymphopoiesis are also involved in malignant B-cell nurturing. Among factors co-expressed by stromal elements within these different specialized niches, we identified the pleiotropic matricellular protein secreted protein acidic and rich in cysteine (SPARC). The actual role of stromal SPARC in normal B-cell lymphopoiesis, investigated in *Sparc*$^{-/-}$ mice and BM chimeras retaining the *Sparc*$^{-/-}$ genotype in host stroma, demonstrated defective BM and splenic B-cell lymphopoiesis. Moreover, in the *Trp53* knockout (KO) lymphoma model, *p53*$^{-/-}$/*Sparc*$^{-/-}$ double-KO mice displayed impaired spontaneous splenic B-cell lymphomagenesis and reduced neoplastic clone BM infiltration in comparison with their *p53*$^{-/-}$/*Sparc*$^{+/+}$ counterparts. Our results are among the first to demonstrate the existence of common stromal programs regulating both the BM osteoblastic niche and the SLO GC lymphopoietic functions potentially fostering the genesis and progression of B-cell malignancies.

Introduction

A tightly regulated cross-talk between hematopoietic cells and mesenchymal stromal cells (MSC) populating the two specialized osteoblastic/endosteal and vascular stromal niches within the bone marrow (BM) maintains homeostatic lymphopoiesis. In secondary lymphoid organs (SLO), mesenchymal stromal cells phenotypically similar to BM resident MSC intervene in the specification of the lymphoid cell fate and the instruction of immune response. Lymphomagenesis, which commonly arises within SLO, is favored in presence of faulty stromal signals. Lymphomatous clones frequently colonize the BM at various

*Correspondence to: Mario Colombo; Email: mario.colombo@istitutotumori.mi.it; Sabina Sangaletti; Email: sabina.sangaletti@istitutotumori.mi.it
Submitted: 04/01/2014; Accepted: 04/23/2014; Published Online: 06/05/2014
Citation: Sangaletti S, Tripodo C, Portararo P, Dugo M, Vitali C, Botti L, Guarnotta C, Cappetti B, Gulino A, Torselli I, et al. Stromal niche communalities underscore the contribution of the matricellular protein SPARC to B-cell development and lymphoid malignancies. OncoImmunology 2014; 3:e28989; http://dx.doi.org/10.4161/onci.28989http://dx.doi.org/10.4161/onci.28989

stages during the course of lymphoma. In the BM, lymphoid clones display specific localization within the specialized BM stromal niches according to their follicular or extra-follicular origin. We hypothesize the existence of common stromal motifs in secondary and primary lymphoid organs that license normal stromal cell function while nurturing transformed lymphoid cells.

The BM osteoblastic niche comprises mesenchymal stromal cells with specific phenotypic profiles, such as CD271$^+$ osterix$^+$ CD146$^+$ and CXCL-12$^+$, which function differentially in the support of hematopoietic stem cells (HSC), common lymphoid progenitor cell maintenance and in the nurturing of B-lymphoid progenitors toward maturation.[1] The early stages of B-cell development in the BM completely depend on stromal cells contacting developing B cells through adhesion molecules and by the production of growth factors and cytokines, such as membrane-bound stem-cell factor (SCF/KITLG)[2] and interleukin-7 (IL-7) acting on late pro-B and pre-B cells, respectively.[3] After the pre-B stage, B-cell maturation becomes progressively less dependent upon contact with stromal cells, until B cells leave the bone marrow to migrate into the SLO and peripheral non-lymphoid tissues toward antigen-driven events.

In the spleen, immature B cells become follicular (FoB) or marginal zone B cells (MZB) through a process that, in part, depends on B-cell receptor (BCR)-mediated signals and that is deeply influenced by the nature of stroma-derived signals.[4] In particular, MZB, which are initially committed by weak BCR signals, more than FoB depend on stroma-derived stimuli, such as the tumor necrosis factor superfamily member BAFF (TNFSF13B) and Notch ligands. These factors contribute to downstream NF-κB activation and cell-fate specification. Similarly to stromal cells of the BM niche, those within SLO are also active in B-cell development. Nevertheless, whether common motifs exist in the two microenvironments and whether common stroma-intrinsic events between these two compartments exert influence on either lymphopoiesis or on the outgrowth of neoplastic clones remains unclear.

Along with soluble factors, stromal cells of primary and secondary lymphoid organs, namely BM mesenchymal stromal cells and follicular dendritic cells, produce insoluble extracellular matrix molecules that both contribute to the stromal scaffolding and exert regulatory functions. These latter functional characteristics depend on the expression of specific receptors recognizing ECM molecules or their fragments on immune cells. Sensing the extracellular matrix and cytoskeletal modifications is important to modulate adhesive dynamics in response to BCR signaling in an antigen-independent fashion.[5] Accordingly, the basement-membrane molecules laminin α5 (LAMA5) and agrin (AGRN) directly foster the differentiation of a specialized population of MZB lymphocytes.[6] This observation supports the idea that aberrant changes in ECM organization might participate in the pathogenic events driving lymphoid malignancies by affecting the development and function of immune cells.[7] Among the relevant modifications occurring in the BM and SLO stromal compartments, we have uncovered the importance of the matricellular protein secreted protein acidic and rich in cysteine SPARC in the homeostatic and pathogenic settings of hematopoiesis and lymphomagenesis, respectively. Specifically, the high expression of SPARC in the stroma plus the pressure of a myeloproliferative spur induces aberrant osteoblastic niche expansion toward myelofibrosis.[8] On the contrary, the absence of stromal SPARC alters the hematopoietic niche favoring myeloid precursor expansion in the BM.[8] In SLO, SPARC deficiency alters the mesenchymal follicular dendritic cells (FDC) networking[9] and, in the case of persistent perturbation of lymphoid tissue homeostasis, impairs humoral immunity while promoting lymphomagenesis.[10] In this latter scenario, the absence of SPARC results in defective collagen assembly and resultant lack of myeloid cell inhibitory signals mediated by the collagen receptor, leukocyte-associated immunoglobulin-like receptor 1 (Lair-1) expressed on myeloid cells, particularly neutrophils. Hyper-activated neutrophils acquire an interferon (IFN)-related signature and eventually die through a type of immune cell death referred to as NETosis that promotes CD5$^+$ B-cell transformation via NF-kB. The emerging scenario indicates that stromal SPARC expression has an indirect effect on lymphomagenesis by controlling the behavior of bystander immune cells rather than influencing CD5$^+$ B cells directly. Specifically, authors found a correlation between reduced microenvironmental SPARC expression and ECM deposition along with signs of NETotic neutrophil among the activated infiltrating myeloid cells in human B cell chronic lymphocytic leukemia (B-CLL).[10]

Overall, these prior data led us to hypothesize that stromal SPARC may represent a common regulatory trait linking hematopoietic and lymphopoietic homeostasis in both BM and SLO niches. In this study, we have investigated the influence of SPARC-defective stroma over the lymphopoietic function of the BM and SLO highlighting a novel function of the extracellular matrix in regulating the equilibrium between the different B-cell precursors and their differentiated progeny, findings which may have implications in lymphoid malignancy specification and disease progression.

Results

The bone marrow osteoblastic niche and SLO follicles display common stromal features

We first sought to investigate whether the stromal composition of the BM and SLO lymphopoietic microenvironment share common elements. To this end, we analyzed the expression of prototypical MSC markers and the levels of key extracellular matrix proteins in human BM samples with or without signs of osteoblastic niche remodelling, and in lymph node and tonsil samples with reactive follicular hyperplasia. As shown in **Figure 1**, immunohistochemical (IHC) analyses showed that the neurotrophin receptor CD271 and the adhesion molecule CD146 were mainly detected in the mesenchymal elements lining the bone trabeculae within the osteoblastic/endosteal compartment of the normal BM parenchyma. The spatial association between BM-MSC marker expression and the osteoblastic niche was further substantiated by the expansion of the stained area in BM samples with signs of active osteoblastic remodelling (**Fig. 1**).

Notably, within SLO, the same markers could be detected in the follicular dendritic cell and reticular cell meshwork of the lymphoid follicles (**Fig. 1**). The link between the BM and SLO mesenchymal architecture was further strengthened by the immunolocalization of CD10, which marks stromal reticular cells preferentially localized in the osteoblastic compartment and scattered B-cell precursors in the BM, and, which also identifies follicular germinal center stromal cells and B cells in SLO (**Fig. 1**). We have recently demonstrated that the matricellular protein SPARC plays a fundamental role in the regulation of mesenchymal organization and extracellular matrix assembly in the BM osteoblastic niche and in the SLO germinal center.[8] In the BM, SPARC stained mesenchymal stromal cells lining the endosteum along with osteoblasts (**Figs. 1 and 2A**), whereas in SLO SPARC identified FDC, GC-associated macrophages, and marginal zone reticular cells with a decreasing density gradient from the GC toward the marginal layers of the follicle (**Figs. 1 and 2B**). Staining for type I collagen and fibronectin, which are SPARC-regulated ECM proteins, identified the same mesenchymal elements populating the osteoblastic niche of the BM and the follicles of SLO (**Fig. 1**). These results suggest that BM and SLO, although differing in the overall cellular composition and function, maintain a high degree of homology in the composition of mesenchymal and extracellular matrix elements of areas hosting B-cell lymphoid precursors and maturating (and plastic) B lymphocytes undergoing early differentiation. Consistent with this premise, SPARC-expressing stromal elements in the BM contacted $CD10^+$ B-cell precursors (**Fig. 2C**), whereas in the spleen they were found associated with IgM^+ B-cells that comprise the transitional B-cell fractions in the follicle center and at the edge of the marginal zone areas (**Fig. 2D**).

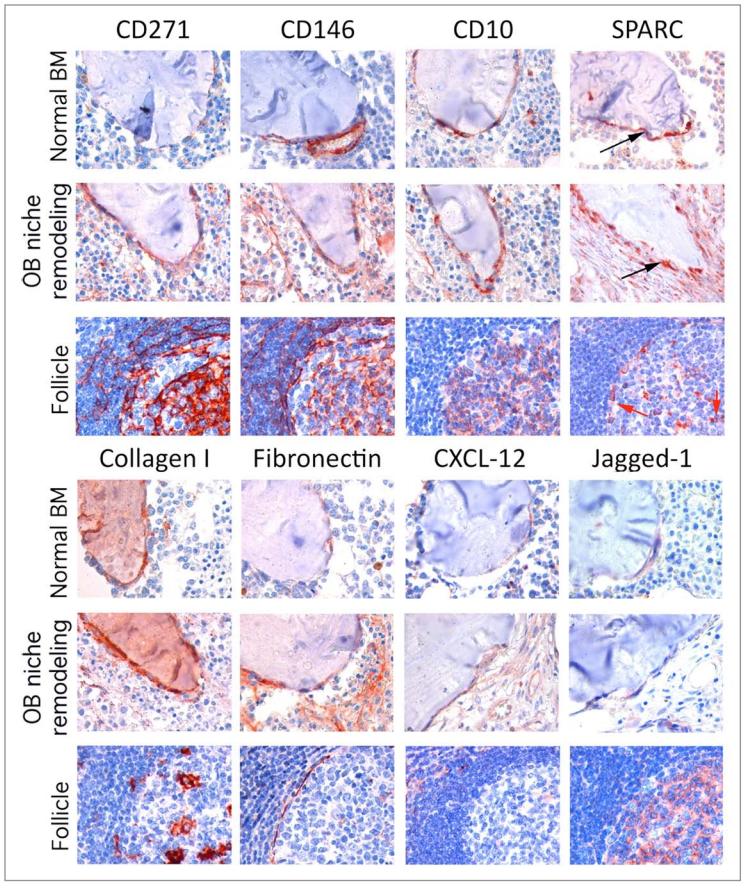

Figure 1. Common mesenchymal features characterize the BM osteoblastic niche and SLO follicles. Representative stainings for CD271, CD146, CD10, secreted protein acidic and rich in cysteine (SPARC), collagen type-I, fibronectin, CXCL12 and Jagged-1 of one normal BM parenchyma, one BM with primary myelofibrosis, as an example of osteoblastic niche remodeling, and one reactive follicular hyperplasia in the SLO (tonsil). These structural and functional stromal cells markers stain mesenchymal cells in the osteoblastic BM niche (black arrows) and follicular dendritic cells and macrophages in SLO follicles (red arrows).

These common features underscore the preferential homing of nascent B cell neoplasms that, although originating in SLO, seed the BM within SPARC-rich areas. Indeed, the histopathological analysis of 197 cases of non-Hodgkin's B-cell lymphoma of centro-follicular origin involving the BM, namely follicular lymphomas and diffuse large B-cell lymphoma of germinal center derivation (including T-cell/histiocyte-rich diffuse large B-cell lymphoma), highlighted a preferential localization of the neoplastic clones to the paratrabecular areas of the osteoblastic niche occurring in 69% of cases (**Fig. 3A and B**). In contrast, clones of extra-follicular derivation, including small lymphocytic lymphoma, marginal zone lymphoma, mantle cell lymphoma, lymphoplasmacytic lymphoma, and non-GC B-cell like diffuse large B-cell lymphoma, seemed to prefer the perivascular area of BM parenchyma and sporadically localized within the paratrabecular areas (**Fig. 3A**) The colonization of paratrabecular areas by lymphoid clones was associated with the expansion of $CD146^+$ MSCs (**Fig. 3C**), upregulation of SPARC (**Fig. 3D**), and expression of the associated ECM proteins fibronectin and type-I collagen (not shown). Of note, such modifications were also found in the less typical localization to the parenchymal vascular niche of centrofollicular clones, suggesting the existence of common mesenchymal cells that are recruited by neoplastic clones in order to reproduce a microenvironment reminiscent of their origin.

SPARC deletion affects the early phases of B-cell development in the bone marrow

In order to test the functional relevance of mesenchymal SPARC commonly expressed within the specialized microenvironments of BM and SLO, we adopted a SPARC-deficient mouse model to assay the consequences of SPARC ablation on B cell lymphopoeisis. First, we set out to validate our model by testing the consistency of SPARC expression in mouse BM mesenchymal cells nurturing B-cell precursors. In the mouse, niches hosting B cells precursors, common lymphocyte progenitors, and hematopoietic stem cells (HSCs) have recently been characterized, and specific gene-expression profiles of the different mesenchymal populations have been obtained.[1] We analyzed *Sparc* expression within these previously published gene expression (GE) profiles of different mesenchymal populations and compared the levels of *Sparc* mRNA to that of the endogenous mesenchymal markers

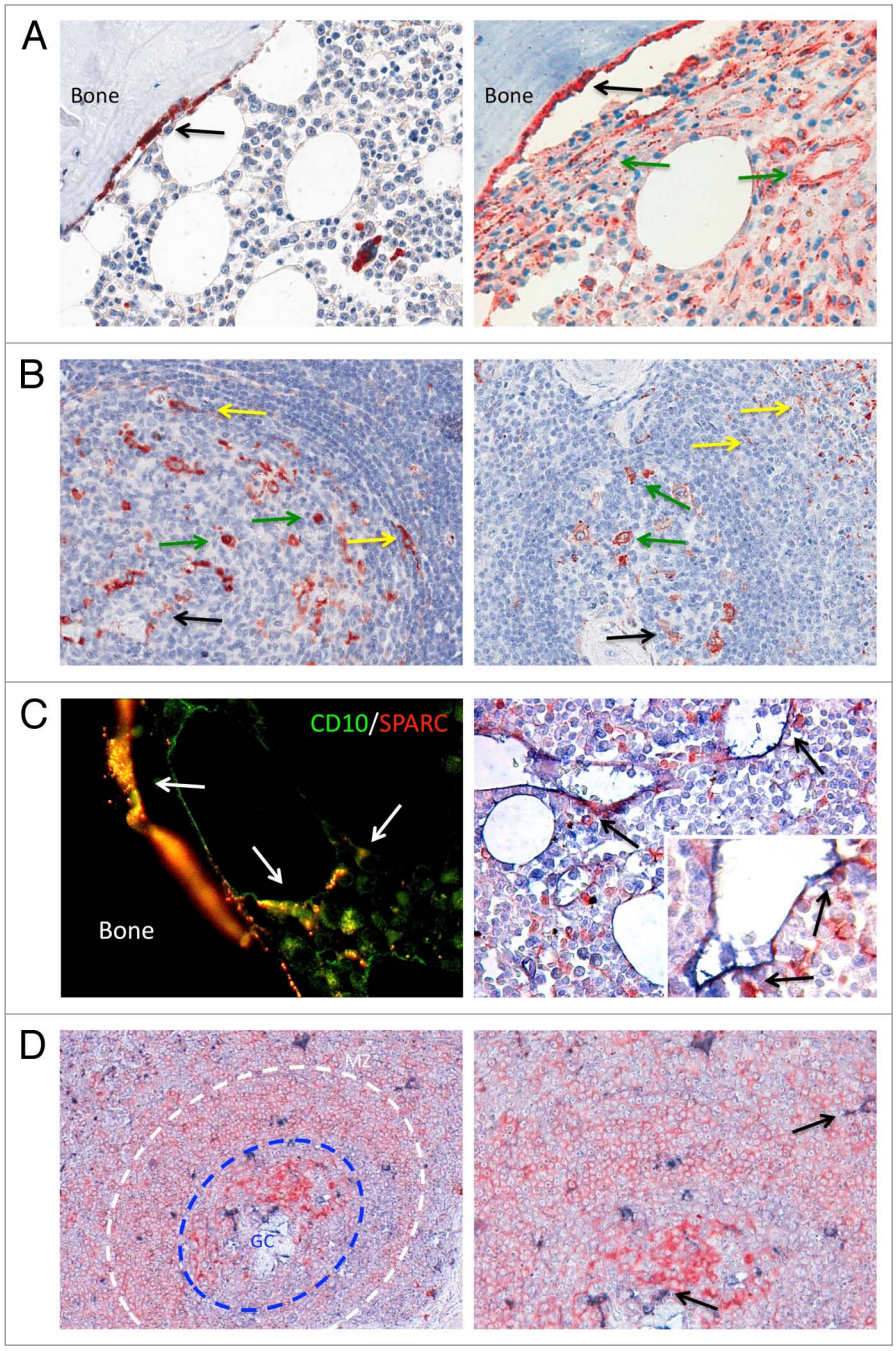

Figure 2. SPARC immunolocalization in mesenchymal elements of human BM and SLO. (**A–D**) Immunohistochemical (IHC) analysis of secreted protein acidic and rich in cysteine (SPARC) expression within the normal bone marrow (BM) and follicles of secondary lymphoid organs (SLO) and their reactive counterparts. Representative microphotographs shown are from one case per condition. (**A**) In the quiescent osteoblastic niche (left panel) SPARC is confined to mesenchymal stromal cells (MSC) lining the endosteum (black arrows). The expression of SPARC is upregulated in the BM with signs of osteoblastic niche remodeling (right panel), where it extends to mesenchymal reticular and subendothelial cells (green arrows). (**B**) In SLO (lymph node, left panel; spleen, right panel), SPARC is expressed by follicular dendritic cells (FDC, black arrows), germinal center (GC)-associated macrophages (green arrows), and reticular cells (yellow arrows) with a density gradient of expression between the GC toward the marginal layers of the follicles. (**C**) Left panel: Double-marker immunofluorescence showing the co-expression of SPARC (red) and CD10^{+} (green) mesenchymal elements in the intact BM osteoblastic niche. Right panel: Double-marker IHC analysis showing that SPARC-expressing CD10^{+} mesenchymal reticular cells contact CD10^{+} B lymphoid precursors within the normal BM parenchyma. (**D**) Normal spleen IHC analysis for SPARC (blue) and IgM (red) showing SPARC-expressing stromal elements contacting IgM^{+} B-cell, which comprise the transitional B-cell fractions, within follicle GC and at the edge of the marginal zone areas.

like CD29 (*Itgb1*), PDGFRα (*Pdgfra*), and Galectin-1 (*Lgals-1*). *Sparc* mRNA was found to be robustly expressed by both BM mesenchymal cell subsets examined, including CXCL12^{+} reticular cells (2 replicate samples) and PDGFRα^{+} Sca^{+} stromal cells, its intensity value being above the upper whisker and above selected positive control genes (**Fig. 4A**). Moreover, immunolocalization analyses performed on paraffin-embedded BM samples from WT BALB/c mice showed that SPARC was expressed by mesenchymal elements and predominantly localized to the para-trabecular areas, in which its association with the osteoblastic niche was demonstrated by co-localization analysis with type-I collagen (**Fig. 4B and C**). These data are confirmative of our human studies, evincing that SPARC expression characterizes BM mesenchymal elements of the stromal niches delegated to nurse hematopoietic precursors, including B-cell progenitors.

To investigate whether defective SPARC expression could affect BM B-cell lymphopoiesis we evaluated B cell development and differentiation in the BM of *Sparc*$^{+/+}$ and *Sparc*$^{-/-}$ mice according to Hardy and collaborators.[11] Flow cytometry analysis of BM cell suspensions showed a reduced fraction of B220^{+} cells in the BM of *Sparc*$^{-/-}$ relative to wild-type (*WT*) mice. Within the B220^{+} B-cell fraction, the most reduced cell population was CD43^{-} B cells, comprising late pre-B and immature B cells, whereas the CD43^{+} fraction was increased (**Fig. 4D–F**).

The analysis of CD24 and BP-1 expression performed within the gate of B220^{+}CD43^{+} cells allowed the identification of various pro-B cell fractions and showed that *Sparc*$^{-/-}$ mouse marrow cells were enriched in fraction A (CD24^{-} BP-1^{-}; pre-pro B cells) whereas they were reduced in fraction B (CD24^{+}, BP-1^{-}: early pro-B cells) (**Fig. 4D and G**). Fractions C (CD24^{low}, BP-1^{+}: late pro-B) and C' (CD24^{high}, BP-1^{+}: early pre-B) were also unbalanced in favor of C, suggesting a block of differentiation in the pro-B phase in SPARC-null mice (**Fig. 4G and H**), further

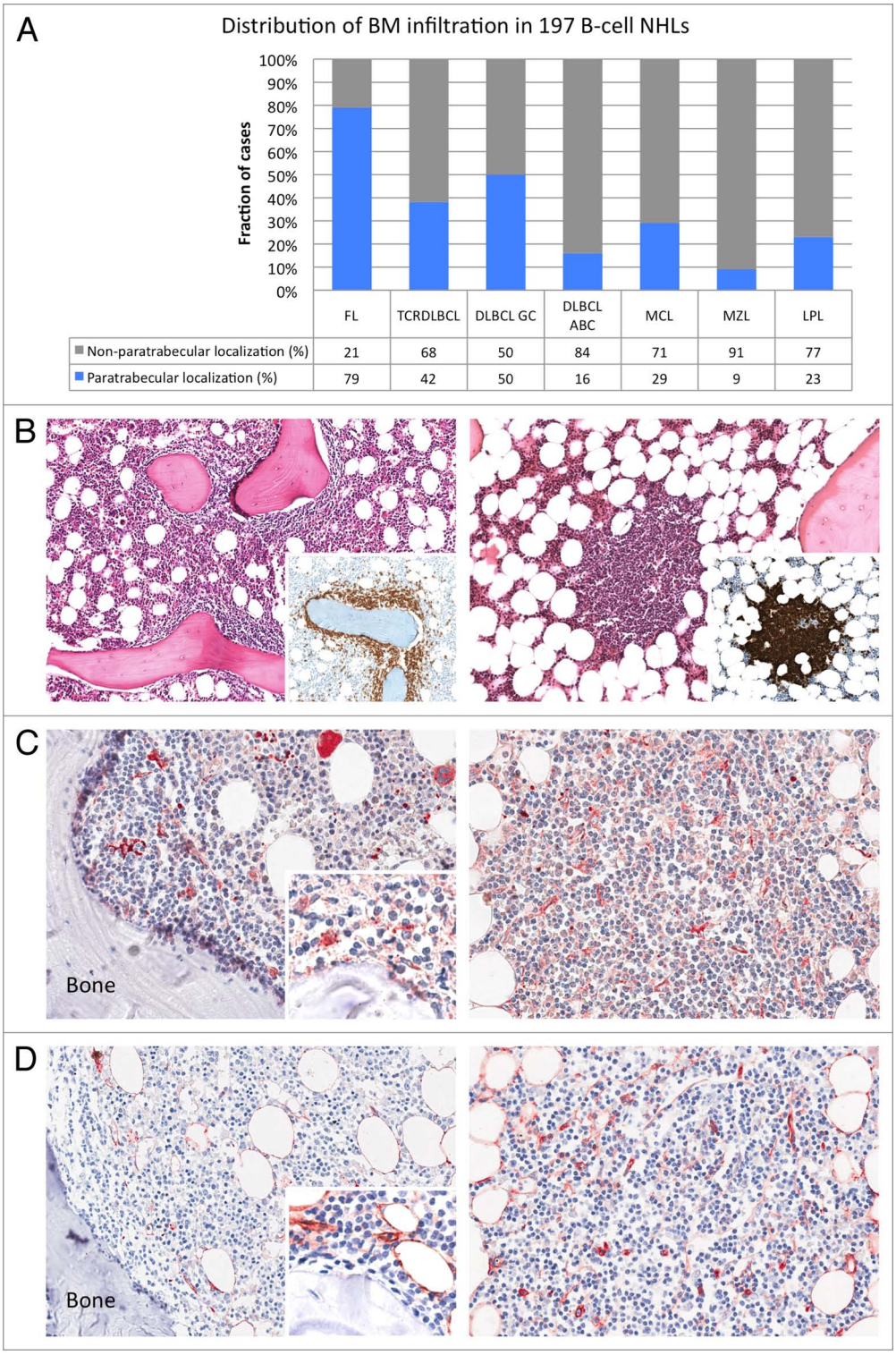

Figure 3. GC-associated lymphoid clones infiltrating the BM osteoblastic niche exhibit mesenchymal features in common with SLO germinal centers. (**A–D**) Histological examination of B-cell non-Hodgkin lymphoma (B-NHL) patient specimens. (**A**) The frequency of para-trabecular/osteoblastic localization of lymphoid malignant clones in 197 cases of B-NHL with bone marrow (BM) infiltration. Lymphoid clones of germinal center (GC)-derivation exhibiting preferential tropism for the BM osteoblastic niche include: follicular lymphoma (FL), T-cell rich histiocyte rich diffuse large B-cell lymphoma (TCRBCL), and diffuse large B-cell lymphoma of GC type (DLBCL-GC). Non-GC-related lymphoid clones include: DLBCL- activated B-cell type (ABC); mantle-cell lymmphoma, (MCL); marginal-zone lymphoma, (MZL); lymphoplasmacytic lymphoma, (LPL). (**B**) Para-trabecular (left panel) and inter-trabecular (right panel) localization of two representative cases of FL with BM infiltration. The distribution of the lymphomatous infiltrates around bone trabeculae or in the inter-trabecular lacunae is highlighted by CD20 immunostaining (inserts). (**C–D**) FL lymphoid infiltrates localizing within the osteoblastic niche area (left panels) and inter-trabecular BM (right panels) display a stromal architecture reminiscent of that of secondary lymphoid organ (SLO) GCs and are characterized by the expression of BM-MSC markers SPARC (**C**) and CD146 (right **D**).

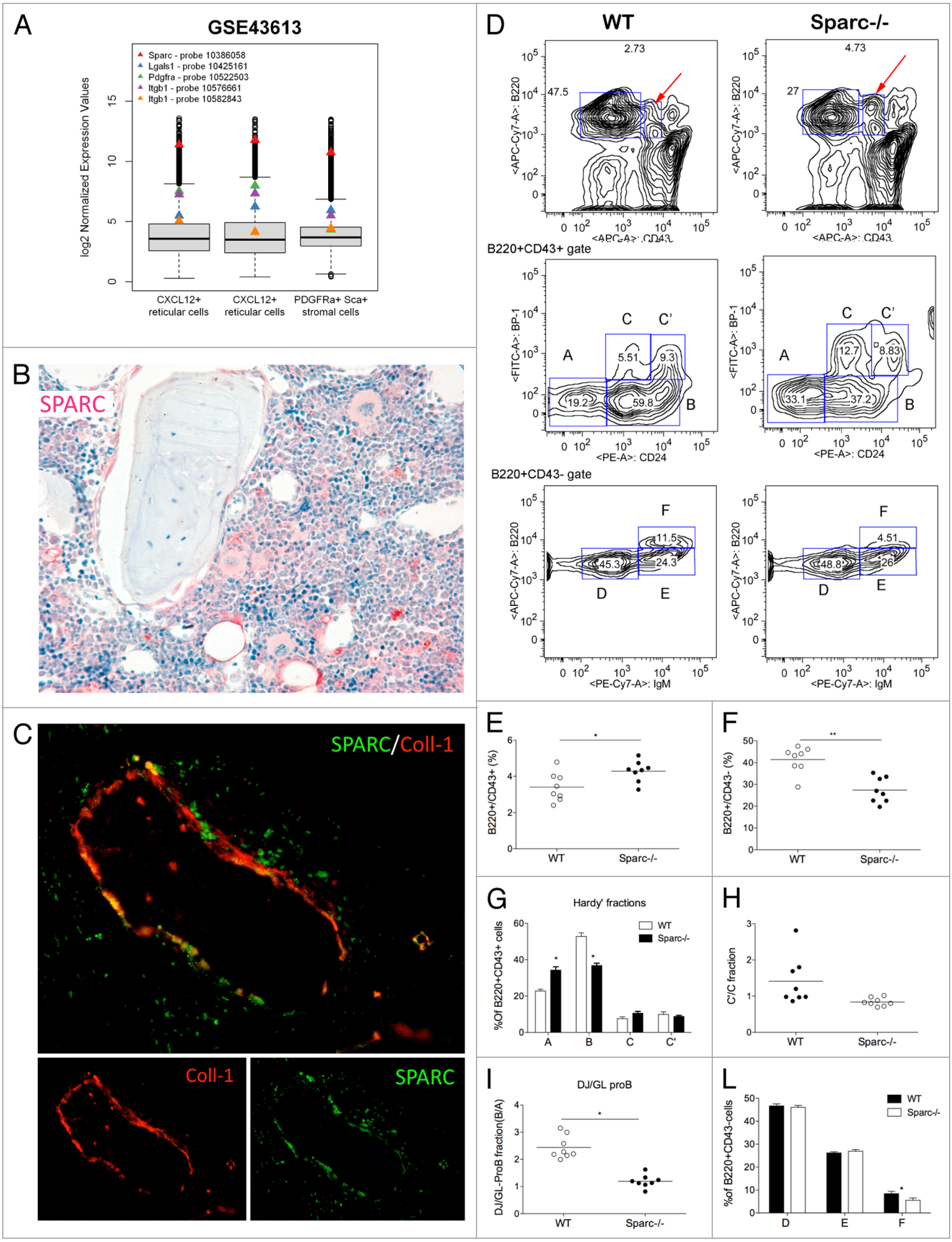

Figure 4. For figure legend, see page 6.

confirmed by the reduction of the DJ/GL-pro-B ratio in the same mice (**Fig. 4I**). Within the decreased CD43$^-$ B cell fraction of Sparc$^{-/-}$ mice, the proportion of fractions D (IgM^{low}, B220$^+$: late pre-B) and E (IgM^{high}, B220$^+$: immature-B cells) was unchanged, whereas the fraction F (IgM^{high}, B220^{high}: recirculating B cells) was reduced in comparison to the *WT* counterpart (**Fig. 4J**). These results underscored an impaired early B-cell differentiation in the absence of the matricellular protein SPARC within the stroma. In support, flow cytometry analysis on B-cell precursors revealed a significant increase in the mean fluorescence intensity (MFI) of the heat-stable antigen CD24 in pro-B and pre-B cells from *Sparc*$^{-/-}$ BM relative to *WT* controls (**Fig. 5A**).

SPARC regulates pro-B cell apoptosis via CD62P-CD24 axis

We have recently shown a correlation between SPARC expression and the modulation of cell death in hematopoietic cells,[10] and further, that SPARC deficiency enhances intrinsic lymphoid B-cell defects associated with mutation of the cell death receptor *Fas* toward lymphoma genesis. The faulty stroma-derived signals due to SPARC deficiency alter the activation and cell death profile of immune cells. Also, we demonstrated a direct correlation between the expression of SPARC and that of Fas in human B-cell lymphoid clones. On these bases, we hypothesized that the block of B cell differentiation occurring in *Sparc*$^{-/-}$ BM could reflect the alteration of the normal blend of anti- and pro-apoptotic stimuli sensed by pre- and pro-B cells within the BM environment. Among the receptors tightly involved in the conveyance of cell-extrinsinc pro-apoptotic signals, CD24 is known to play a key role. This small heavily glycosylated cell-surface protein works as receptor for P-selectin (CD62P) to activate apoptosis as a quality checkpoint in B-cell development.[12]

To test the hypothesis of defective SPARC expression influencing B-cell apoptosis via CD24, we evaluated Annexin V binding, an apoptotic marker, within the different lymphoid populations identified by B220, CD43, BP-1, IgM, and CD24 markers. According to CD24 expression, we found that the Annexin V MFI was higher in pro-B and early pre-B cell fractions within *Sparc*$^{-/-}$ mice relative to the *WT* counterpart (**Fig. 5B and C**). The higher Annexin V MFI of *Sparc*$^{-/-}$ mice was also associated with an increased frequency of Annexin V$^+$ cells within the pro-B and early pre-B cells fractions (**Fig. 5D**).

Of note, in WT mice the higher frequency of apoptotic cells occurs in the pro-B fraction (B, C) and decreases progressively from fraction D toward fractions E and F (**Fig. 5B–D**). These data are in line with the notion that late pre-B cells (fraction D) become stroma independent as they acquire dependency on BCR-derived signals during differentiation,[13] which implies escape of CD24-induced apoptosis.[14] Hence, only stroma-dependent pro-B cells are heavily influenced by CD24-mediated apoptosis. Accordingly, *Sparc*$^{-/-}$ mice, which showed higher CD24 expression in B-cell precursor fractions, also showed increased apoptosis limited to the stroma-dependent pro-B cell subpopulation.

Based on the identification of CD62P as a ligand for CD24,[15] we evaluated its expression in the BM of *WT* and *Sparc*$^{-/-}$ mice and found that CD62P expression in BM mesenchymal elements (i.e., endothelial and reticular stromal cells) correlated with the degree of CD24 expression and with B cell precursor apoptosis, being higher in *Sparc*$^{-/-}$ *vs. WT* mice (**Fig. 5E**). These data support the role of SPARC in early B-cell development, conditioning the apoptosis of pro-B cells via the CD24-CD62P pairing.

Although these data may explain the mechanisms for the reduced number of CD43$^-$ cell fraction in the BM of *Sparc*$^{-/-}$ mice, they do not provide an explanation for the concomitant increase in the CD43$^+$ B-cell fraction in the same samples. A plausible explanation may be found in the possible negative regulatory effect exerted by extracellular collagen, which is defective in the *Sparc*$^{-/-}$ precursor niche, on the proliferation of B-cell precursors, as we have already demonstrated for other HSC in the BM niche.[8] Accordingly, the leukocyte-associated immunoglobulin-like receptor 1 (Lair-1), a collagen receptor with inhibitory activity that is not expressed in mature murine B cells,[16] was found to be expressed in CD43$^+$ B cell precursors (data not shown), suggesting that extracellular matrix (ECM) sensing through Lair-1 might affect B-cell precursor quiescence along their stroma-dependent maturation.

WT and *Sparc*$^{-/-}$ bone marrow chimeras confirm the role of stromal SPARC in B-cell development

Our findings of SPARC expression in mesenchymal stromal cells and hematopoietic cells (i.e., megakaryocytes) in the BM parenchyma along with the demonstration of SPARC deficiency affecting the early stroma-dependent phases of B-cell development were strongly suggestive of SPARC participating into the functional composition of the stromal niche hosting lymphoid

Figure 4 (See opposite page). SPARC is expressed by BM-stromal cells and affects the early stages of B-cell lymphopoiesis. (**A**) Normalized gene expression data were downloaded from NCBI's Gene Expression Omnibus (www.ncbi.nlm.nih.gov/geo; accession, GSE43613). Secreted protein acidic and rich in cysteine (*Sparc)* mRNA expression was evaluated in comparison with known mesenchymal-expressed genes (*Itgb1*, *Lgals1*, *Pdgfra*) in CXCL12$^+$ reticular cells (2 replicate samples) and PDGFRα^+ Sca$^+$ stromal cells. The box plot shows the distribution of normalized gene expression intensities for each sample. The bottom and top of the box are the first and third quartiles respectively, and the line inside the box is the median value. Whiskers extend from the box to 1.5 times the difference between the third and the first quartile (interquartile range). *Sparc,* red triangle; *Lgals1*, blue; *Pdgfra*, green; *Itgb1*, purple and orange). (**B**) Representative immunohistochemical analysis showing mesenchymal SPARC expression predominantly localized to paratrabecular areas in bone marrow (BM) samples in wild-type (WT) mice. (**C**) Representative immunofluorescence microscopy analysis showing SPARC (red) and collagen type-I (coll-1; green) colocalization in mesenchymal paratrabecular elements in the BM of WT mice. (**D–H**) Cyofluorimetric analysis of the frequency of CD43$^+$ and CD43$^-$ B-cell in the BM of WT and *Sparc*$^{-/-}$ mice (n = 8/group) as well as the Hardy's profile analysis performed within the B220$^+$CD43$^+$ gate (red arrows). BM cells were stained with fluorophore-conjugated antibodies against the indicated marker and analyzed by flow cytometry. (**D**) Representative contour plots. Collective data obtained from the analysis of 8 mice/group and showing the percentage of B220$^+$CD43$^+$ (**E**), B220$^+$CD43$^-$ (**F**) cells or the percentage of the A, B, C and C′ Hardy's fractions (**G**). (**H**) Ratio between C′ and C fraction within the B220$^+$CD43$^+$ cell subset in the presence and absence of SPARC. (**I**) Ratio between DJ and GL-ProB cells that was also reduced in the absence of SPARC; (*P < 0,05; Student t test). (**J**) Collective data showing the percentage of fraction D,E,F in the B220$^+$CD43$^-$ cell subset. All these results are from one of 3 independent experiments with similar results (8 mice/group for each experiment). Statistical analyses were performed by Student's test; *P < 0.05 and **P < 0.01.

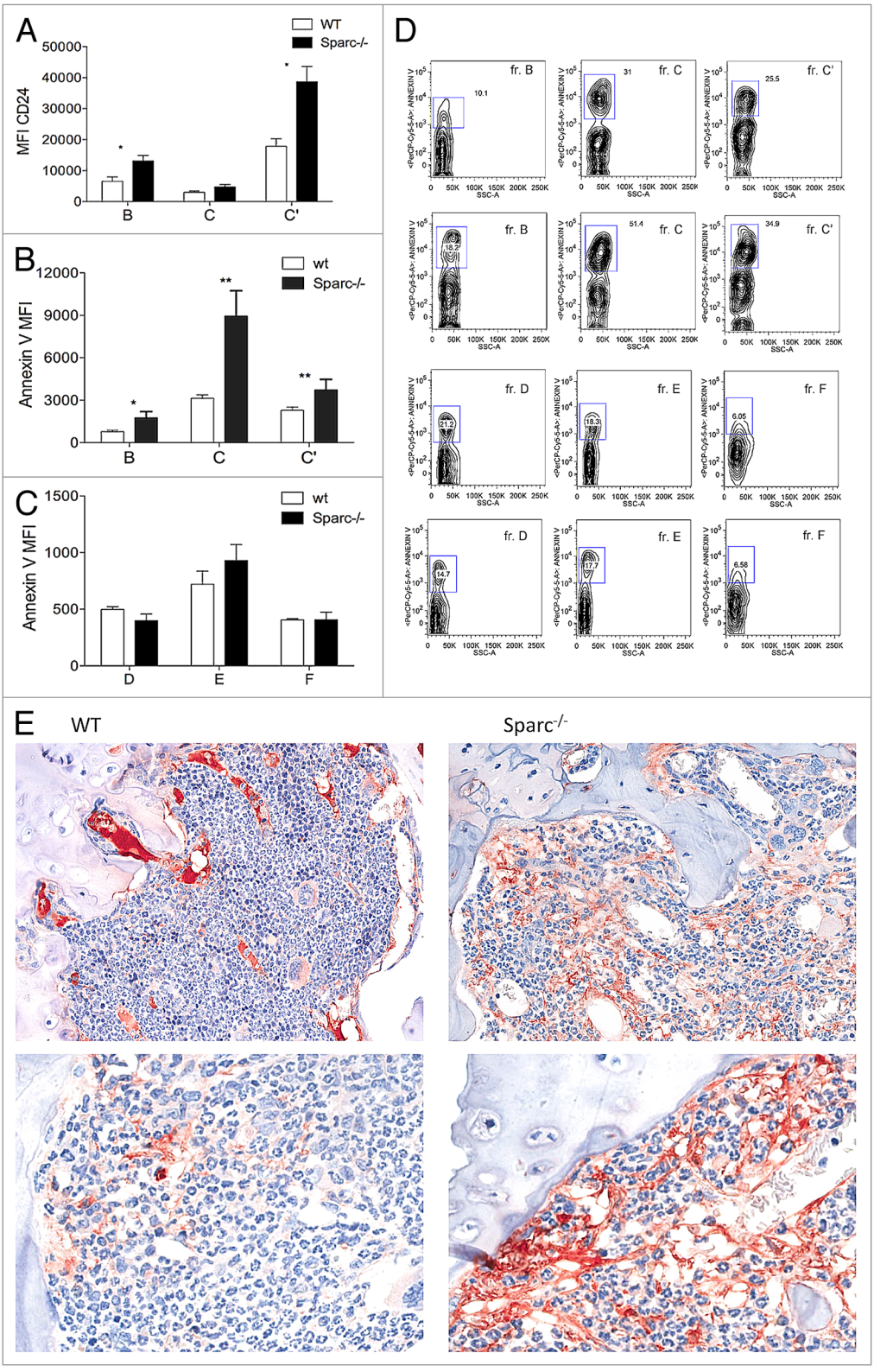

Figure 5. Enhanced expression of CD62P and CD24 is associated with increased pre-B cell apoptosis in Sparc$^{-/-}$ mice. (**A–D**) Cyofluorimetric analysis of B-cell precursors present in the bone marrow (BM) of *Sparc*$^{-/-}$ vs. wild-type (*WT)* control mice (n = 8/group). BM cells were stained with fluorophore-conjugated antibodies against the indicated marker and analyzed by flow cytometry. Results shown are from one of 3 independent experiments with similar results. (**A**) Cumulative data showing CD24 expression (mean fluorescence intensity = MFI) on Hardy's fractions B, C and C' (early pro-B cells, late pro-B and early pre-B). (**B**) Annexin V binding within various pro B-cell populations. (**C**) Annexin V binding within various pre-B cell populations (fraction D, E and F). (**D**) Representative contour plot showing the increased percentage of Annexin V positive cells within the pro-B and early pre-B cell fractions of *Sparc*$^{-/-}$ mice in comparison to *WT* mice. (**E**) Representative IHC analysis of BM mesenchymal CD62P expression in *Sparc*$^{-/-}$ *vs. WT* mice , at different magnification..

progenitors and B cell precursors. To further verify this hypothesis and assess whether mesenchymal cells are the source of SPARC responsible for B-cell modulation, we performed bone marrow transplantation (BMT) experiments in order to derive chimeric mice with radioresistant recipient-derived BM mesenchyma either deficient or proficient for SPARC and donor-derived hematopoietic cells of the reciprocal *Sparc* genotype.[8,17]

We found that *Sparc*$^{-/-}$ recipients, regardless of the *Sparc* genotype of donor lineage negative (Lin$^-$) cells, showed a reduction in B220$^+$CD43$^-$ cells and a block in the pro-B phase of B-cell differentiation in the BM (**Fig. 6A–F**). Similarly to *Sparc*$^{-/-}$ mice, WT > *Sparc*$^{-/-}$ chimeras showed increased expression of CD24 in B220$^+$ cells that was dependent on SPARC deficiency in mesenchymal cells. Indeed, the MFI of CD24 on pro-B and pre-B cells was higher in WT > *Sparc*$^{-/-}$ and *Sparc*$^{-/-}$ > *Sparc*$^{-/-}$ than in reciprocal *Sparc*$^{-/-}$ > WT and WT > WT chimeras (**Fig. 6F**). Also the expression of the CD24 ligand, CD62P similarly varied according to the *Sparc* genotype of BM stroma, with a higher expression level in the absence of mesenchymal SPARC (**Fig. 6G**).

The role of SPARC in the dynamic crosstalk between stromal cells and B cell progenitors was demonstrated using secondary BMT experiments (**Fig. 7**). Lin$^-$ cells were obtained from WT > *Sparc*$^{-/-}$ and *Sparc*$^{-/-}$ > WT chimeras and re-transplanted into WT or *Sparc*$^{-/-}$ recipients. As a read out, we evaluated the fractions of B220$^+$CD43$^+$ and B220$^+$CD43$^-$ cells within the BM. WT Lin$^-$ cells that in primary WT > *Sparc*$^{-/-}$ BMT showed impaired B220$^+$CD43$^-$ B-cell fraction, were able to normally reconstitute this B-cell fraction when injected into WT recipients but not upon transplantation in *Sparc*$^{-/-}$secondary recipients. These remarkable results demonstrate for the first time in vivo, that "re-education" of lymphoid progenitors is contingent upon stroma-derived SPARC. Confirmatory results were obtained transplanting *Sparc*$^{-/-}$Lin- cells from *Sparc*$^{-/-}$ > WT chimeras into *Sparc*$^{-/-}$or WT mice. Indeed, *Sparc*$^{-/-}$ HSC primed in a SPARC-competent environment and gaining the capacity to form a normal B220$^+$CD43$^-$ fraction lost such capacity when re-transplanted into *Sparc*$^{-/-}$ recipients (**Fig. 7**).

In conclusion, these data show that stroma-derived SPARC is crucial to the functional organization of the BM mesenchymal niches hosting B cell precursors and participating in complete B-cell development.

SPARC effects B-cell maturation in the spleen

The high degree of homology between BM and SLO B-cell niches suggested investigating whether the defective expression of SPARC could also affect peripheral splenic B-cell lymphopoiesis. Accordingly, other ECM molecules such as laminin α5 and agrin influence marginal zone B (MZB) lymphocyte differentiation regulating their localization within the splenic niches hosting immature B cells.[6]

We evaluated whether CD93$^+$ immature B cells[18] circulating out from the BM into the spleen are lodged within mesenchymal cell niches characterized by the expression of SPARC and other related ECM molecules, such as collagen type IV. We found CD93$^+$ cells interlaced with collagen IV fibers produced by mesenchymal cells that also make SPARC and localize at the edge of the follicle and within the marginal zone areas (**Fig. 8A**). This observation suggests that SPARC produced by SLO mesenchymal cells takes part in peripheral B-cell development,. Splenic B-lymphopoiesis was characterized in both *WT* and *Sparc*$^{-/-}$ mice by flow cytometry staining with monoclonal antibodies (mAbs) to CD19, B220, CD93, IgD, IgM, CD23, CD21/35. *Sparc*$^{-/-}$ mice were characterized by an overall reduction in the fraction of splenic immature B cells (B220$^+$CD93$^+$) and in that of transitional T1 lymphocytes (**Fig. 8B–E**). This phenotype was phenocopied by WT > *Sparc*$^{-/-}$ BM chimeras, where the *Sparc* genotype of the recipient stroma dictated the fate of immature B cells (not shown). Moreover, in the BM chimeras, defective B-cell development was enhanced in case of *Sparc*$^{-/-}$ recipients, irrespective of the donor SPARC genotype. Indeed, 8 wk post-BMT, the percentage of total B cells was dramatically reduced in comparison to *WT* recipients. According to the pro-homeostatic functions of SPARC,[19] its absence, specifically in the mesenchymal compartment, impairs B-cell maturation.

Further analysis showed that SPARC also affect the repartition of B-lymphocytes between the follicular and the marginal zone fate in favor of the latter (**Fig. 8F and G**). Splenic marginal zone differentiation depends on microenvironmental signals conveyed to B cells through the NOTCH-2/Delta like-1 (Dll-1) pathway. We found increased NOTCH signaling in *Sparc*$^{-/-}$ splenic B cells than in the *WT* counterpart (**Fig. 8H**). This was associated with a more intense and diffuse expression of DLL-1 (not shown). Cytofluorimetric analysis revealed that DLL-1 was produced by myeloid cells, including F4/80+ macrophages and unexpectedly CD11b$^+$GR-1$^+$ neutrophils (**Fig. 8I**), which more copiously infiltrated the spleen of *Sparc*$^{-/-}$ mice (not shown) and which have recently been shown to be endowed of B-cell helper functions.[20] In the spleen, neutrophils localize in the marginal zone area, and are thus favored for contact with MZB by the absence of SPARC (**Fig. 8L**). Nevertheless, the imbalance in the follicular/marginal B-cell ratio occurring in *Sparc*$^{-/-}$ mice did not change the efficacy of marginal zone responses to specific T-independent antigens (p-nitrophenyl phosphate [NPP]-Ficoll; data not shown).

Stromal SPARC deficiency reduces the incidence of spontaneous splenic and BM infiltrating B-cell lymphomas occurring in p53$^{-/-}$ mice

To test whether defective lymphopoiesis resulting from mesenchymal SPARC deficiency also affect lymphomagenesis, *p53*$^{-/-}$ mice were rendered SPARC deficient by genetic crossing. The histological type and frequency of spontaneous splenic B-cell lymphomas arising in *p53*$^{-/-}$ mice was determined according to Morse and colleagues[21] also combining histopathological and immunophenotypical analyses. Additional flow cytometry analysis was performed to assess the expression of specific B-cell markers associated with an increased forward angle light scatter (FSC) contrasting with that of normal B cells exhibiting low FSC.[22] Histological analysis showed that among the cohort of *p53*$^{-/-}$ mice analyzed, ~30% developed reactive follicular hyperplasia, ~40% splenic follicular lymphoma (FL), ~10% developed a marginal zone hyperplasia or splenic marginal zone lymphoma (MZL), ~10% were diagnosed with splenic mantle cell lymphoma, and ~10% with peripheral T-cell lymphoma. Representative flow cytometry analysis of *p53*$^{-/-}$ cases diagnosed with FL or MZL

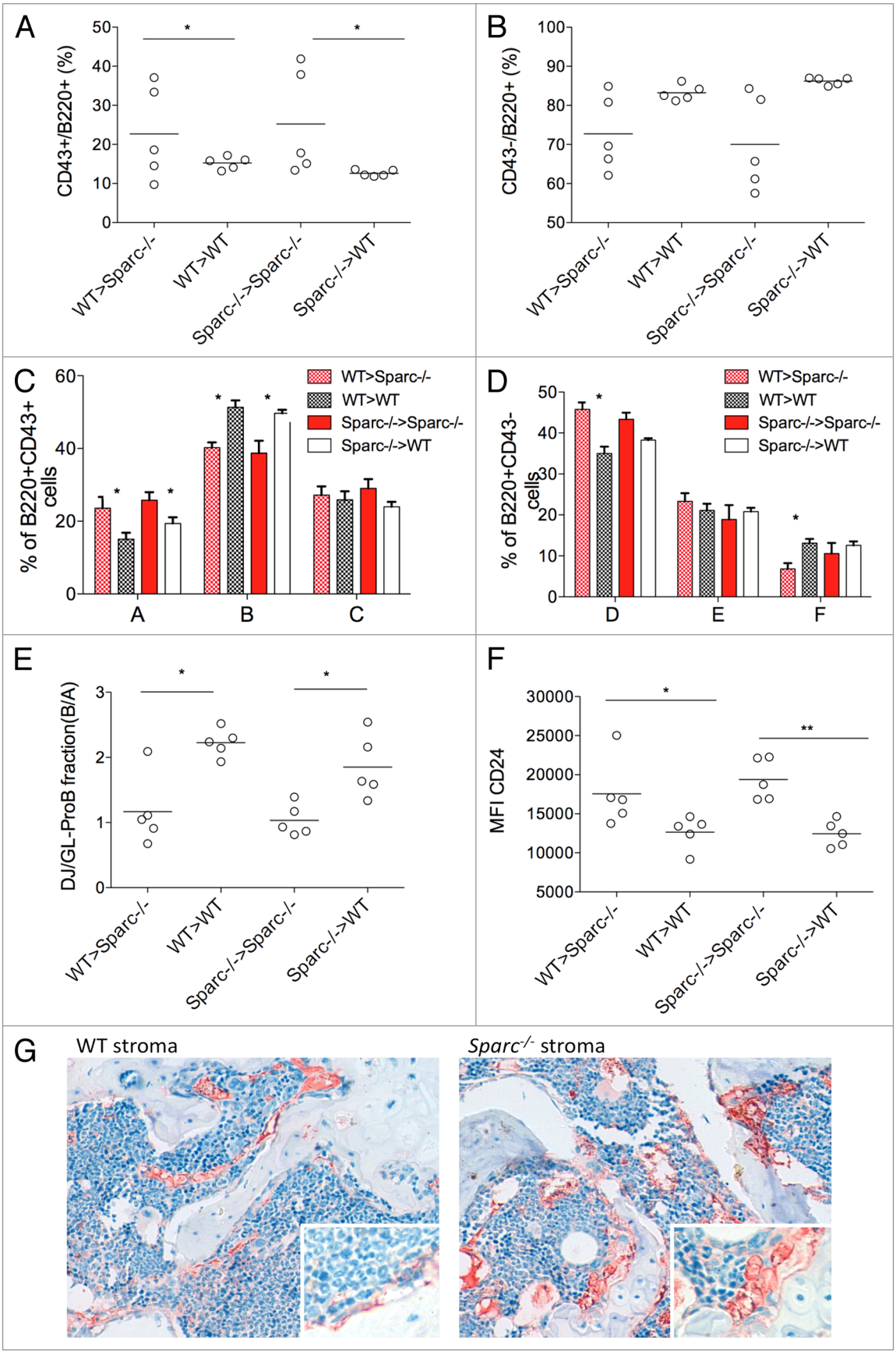

Figure 6. For figure legend, see page 11.

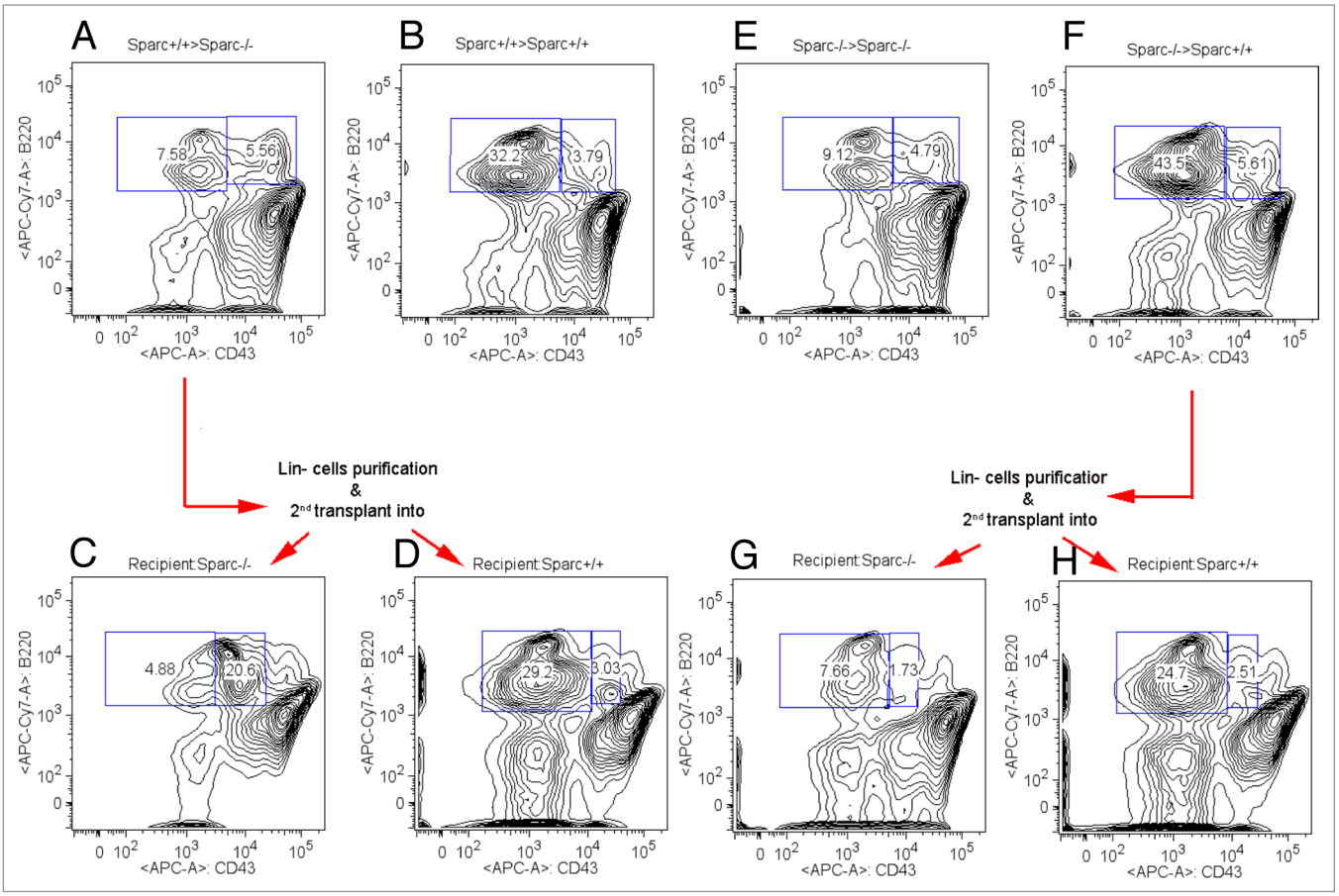

Figure 7. Lymphoid progenitor cell "re-education" depends on stroma-derived SPARC. (**A–H**) We established secondary bone marrow transplantation (BMT) experiments in which lineage negative (Lin^-) cells were obtained from WT > *Sparc*$^{-/-}$ and *Sparc*$^{-/-}$ > WT chimeras, that showed affected or normal B-cell development, respectively, and were re-transplanted into WT or *Sparc*$^{-/-}$ recipients (n = 5 mice/group). We evaluated the fractions of $B220^+CD43^+$ and $B220^+CD43^-$ cells within the BM 8-wks after BMT via flow cytometry (as in **Figure 6** legend). Representative contour plots from the FACS analyses are shown, with arrows indicating the transplantation donors to recipients. (**A–D**) Lin^- cells isolated from WT > *Sparc*$^{-/-}$ donors (panel **A**) remained defective in generating $B220^+CD43^-$ B cells when injected into *Sparc*$^{-/-}$ secondary recipents (**C**) but not when injected into WT recipient (**D**), with a percentage of $B220^+CD43^-$ cells similar to that of control WT > WT mice (**B**). (**E–H**) Lin^- cells isolated from *Sparc*$^{-/-}$ > WT recipients (**F**) underwent normal B cell development when injected into WT recipients (**G**) but not when injected into *Sparc*$^{-/-}$ recipients (**H**) a condition that was similar to that of *Sparc*$^{-/-}$ > *Sparc*$^{-/-}$ chimeras (**E**). The experiments were repeated 2 times with similar results achieved.

are shown in **Figure 9B**, as indicated. Accordingly, most of these mice showed BM enrichment of the same populations that were expanded in the spleen (**Fig. 9A–C**) and displayed infiltration patterns similar to those of their human counterparts. Indeed, BM infiltration exerted by FL and DLBCL (with centroblastic morphology) mainly showed a para-trabecular BM localization, whereas SMZL displayed a prominent intra-sinusoidal and interstitial infiltration.[23] According to their potential splenic origin, these cells were detected within fraction F of the $B220^+IgM^+CD43^-$ BM subset, which normally comprises splenic recycling B cells (**Fig. 9D**). When compared with *p53*$^{-/-}$ mice, the *p53*$^{-/-}$/*Sparc*$^{-/-}$ double mutant mice exhibited a reduced overall frequency of splenic follicular and marginal zone lymphomas and a marked reduction in the frequency of BM infiltration (**Fig. 9A–D**; **Table 1**). The few *p53*$^{-/-}$/*Sparc*$^{-/-}$ splenic lymphomas, that rarely infiltrate the BM were of $B220^+CD23^-CD21/35^+IgM^+$

Figure 6 (See opposite page). WT > *Sparc*$^{-/-}$ bone marrow chimeras phenocopy defective B-cell development occurring in *Sparc*$^{-/-}$ mice. (**A–G**) Cyofluorimetric analysis of B-cell precursors in the bone marrow (BM) of various chimeras derived from transplantion of marrow cells from *Sparc*$^{-/-}$ vs. wild-type (*WT*) mice into the indicated recipient (n = 5/group, except for panel G with n = 3/group). BM cells from each chimera were stained with fluorophore-conjugated antibodies against the indicated marker and analyzed by flow cytometry. Results shown are from one of 3 independent experiments (unless otherwise indicated) with similar results achieved. (**A–B**) Hardy's profile analysis performed on bone marrow (BM) cells from WT > *Sparc*$^{-/-}$, WT > WT, *Sparc*$^{-/-}$ > *Sparc*$^{-/-}$ and *Sparc*$^{-/-}$ > WT BM chimeras. Collective data showing the fraction of $B220^+CD43^+$ B-cells (**A**) and of $B220^+CD43^-$ cells (**B**) in the BM of the different mouse chimeras **C**. Analysis of CD24 and BP-1 performed within the gate of $B220^+CD43^+$ cells showing the increased fraction A and reduced fraction B in *Sparc*$^{-/-}$ recipients (**D**) Collective data showing the frequency of the fraction's D, E, and F calculated within the gate of $B220^+CD43^-$ cells in the BM of chimeric mice. (**E**) Reduced ratio between DJ and GL-Pro B cells (fraction B/fraction A) in *Sparc*$^{-/-}$ recipients. (**F**) Variation of CD24 mean fluorescence intensity (MFI) according to the SPARC genotype of recipient mice. (**G**) CD62P expression in BM-MSC varies according to the *Sparc* genotype of recipient mice.

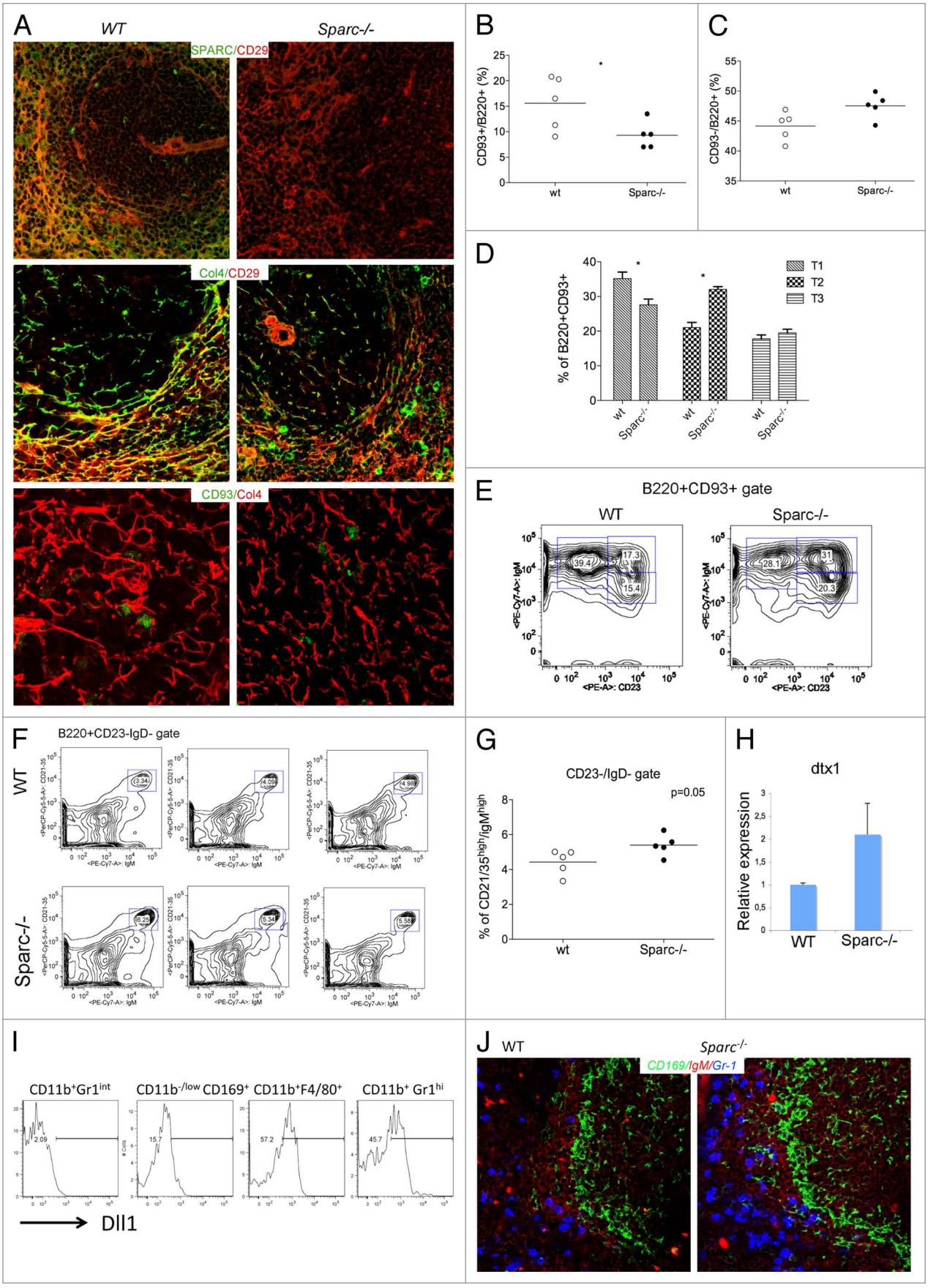

Figure 8. For figure legend, see page 13.

MZB phenotype and were characterized for reduction of CD24. CD24 downregulation could be a strategy to avoid apoptosis triggered by CD62P that is highly expressed in the BM milieu of *Sparc*$^{-/-}$ mice (**Fig. 9D**).

Discussion

To our knowledge this is the first investigation showing the existence of common stromal motifs in primary and secondary lymphoid organs that could systematically regulate normal B-cell development and exert influence over malignant lymphoid transformation. We have demonstrated that the matricellular protein SPARC is relevant to the maintenance of normal lymphopoietic function in the BM and SLO where it functions to regulate the stroma-dependent nurturing of immature pre-B cells. Among stromal factors sharing SPARC involvement in the composition of SLO and BM lymphopoietic niches, we have identified previously characterized co-regulated molecules, including collagen type-I[17] and fibronectin.[24] In our prior work, we demonstrated that these ECM components play an important homeostatic role in the function of two specialized hematopoietic microenvironments with high cellular turnover, namely the BM hematopoietic niche and the SLO germinal center.[8,9] Moreover, our findings suggest that these ECM proteins exert underestimated regulatory function on immune cell activity under physiological and pathological conditions.[10,25] On these bases, we have recently demonstrated that altered ECM organization associated with deficiency of the stromal regulator SPARC is sufficient to foster persistent pro-inflammatory conditions engendering unrestrained interactions between immune cells toward autoimmunity-associated B-cell lymphomagenesis. Yet, little is known about the mechanisms through which ECM molecules can regulate B lymphoid development, fate specification, and transformation.[6] The conventional notion is that tumors originate from the accumulation of mutations in tumor-initiating cells. Recently, it has become increasingly recognized that the cross-talk between neoplastic cells and the stromal microenvironment also plays a fundamental role throughout tumorigenesis, from the earliest stages of establishment, through to tumor maintenance and disease progression. In this context, the role of the stromal microenvironment in hematologic malignancies is less well understood.[26] In lymphoid malignancies, different degrees of relationship exist within the tumor-associated microenvironment that can be identified according to the biology of the malignant clone. Indeed, lymphoid clones with aggressive pace such as Burkitt's lymphoma and some DLBCL, usually display defective receptor machineries and limited reliance on environment-derived signals, in accordance to their dodging of mature-B-cell programs in favor of proliferative programs typical of B-cell precursors.[27] On the other hand, most indolent B-cell clones, such as FL, CLL, and splenic MZL are variably sustained by their multifaceted microenvironment in magnifying the intrinsic imbalance between pro- and anti-apoptotic programs. Here, we have identified a new level of stroma regulation of B lymphopoiesis which relies on the existence of redundant stromal ECM-related motifs in BM and SLO lymphopoietic niches, and, that may also represent a structural tuner of malignant lymphoid cell trafficking among these tissues. Indeed, lymphomas that arise in SLO and colonize the BM at different stages of disease progression display a specific tropism for BM stromal niches, which can be explained by the existence of common pro-survival, supportive niches. These pathological dynamics may reproduce those used by normal B cells to interact with the mesenchymal compartment. The relevance of ECM molecules in such an interaction was proven by our findings that SPARC deficiency altered the fitness of B-cell precursors in the BM and SLO, culminating in impaired normal B-cell development. The relevance of extracellular matrix composition in the lymphopoietic function of BM stromal niches is corroborated by the observation that osteopontin-null mice share with *Sparc* knockout mice an overall decrease in the percentage of B220^{+} cells and a defective pre-B cell development (not shown). Osteopontin, like SPARC, belongs to the class of matricellular proteins[19] that take part in the composition of the BM osteoblastic niche,[28] impacting HSC and tumor cell migration and proliferation.[29,30]

Among molecules identified in hematopoietic cells found to correlate with stromal SPARC expression is the adhesion receptor CD24. Expression of CD24 has been reported in a variety of human epithelial cancers. CD24 may be of prognostic significance since it has been implicated in the trans-endothelial migration of cancer cells and in the constitution of the cancer cell stem-like phenotype, making CD24 a candidate sensor for important environment-related signals in critical precursor cell subsets. The tight link between cell-adhesion signals and the modulation of cell death rescue or induction programs is common to molecules involved in the cross-talk between immune cells and the endothelium, including CD44, CD54, and the

Figure 8 (See opposite page). Stromal-SPARC influence on splenic B-cell maturation. Spleen cells were stained with fluorophore-conjugated antibodies against the indicated marker and analyzed by flow cytometry. (**A**) Confocal microscopy analysis for SPARC, CD29, collagen type-4 (Col4) and CD93 expression in spleens from wild-type (WT) and *Sparc*$^{-/-}$ mice. (**B–C**) Flow cytometric analysis showing the fraction of B220^{+}CD93^{+} (**B**) and B220^{+}CD93^{-} (**C**) cells in the spleen of *Sparc*$^{-/-}$ in comparison to WT mice. (**D–E**) Immature B220^{+}CD93^{+} B cells were classified by immunostaining and cytofluorimetric analysis into transitional T1, T2, and T3 cells based on their expression of CD23 and IgM (T1 = IgM^{+} CD23^{-}, T2 = IgM^{+}CD23^{+}, T3 = IgM^{low}CD23^{+}). (**D**) Collective data for transitional T1, T2 and T3 cells obtained from the analysis of spleen cell suspensions from 5 WT and 5 *Sparc*$^{-/-}$ mice (n = 5 mice/group; Statistical analysis performed by Student's *t* test; **P* < 0.05; ***P* < 0.01; one representative experiment out of 3). (**E**) Representative contour plots for transitional T1, T2 and T3 cells in WT and *Sparc*$^{-/-}$ mice. (**F**) Marginal zone B (MZB) cells were defined within the gate of B220^{+}CD23^{-}IgD^{-} based on their of high level of CD21/35 and IgM. (**G**) Cumulative data showing the frequency of MZB cells in WT and *Sparc*$^{-/-}$ (n = 5 mice/group; one representative experiment out of 3) (**H**) Quantitative RT-PCR analysis for deltex-1 (*Dtx-1)* mRNA expression performed on total CD19^{+} cells sorted from the spleen of WT and *Sparc*$^{-/-}$ mice (n = 3 mice/group). (**I**) Delta-like protein 1 (Dll-1) expression analyzed by flow cytometry in the different myeloid cell subsets defined by the markers CD11b, F4/80 Gr-1 and CD169. (One representative experiment out of 3.) (**J**) Confocal microscopy analysis showing neutrophils localizing to the marginal area, defined by CD169^{+} marginal zone macrophages, and contacting IgM^{high} MZB cells.

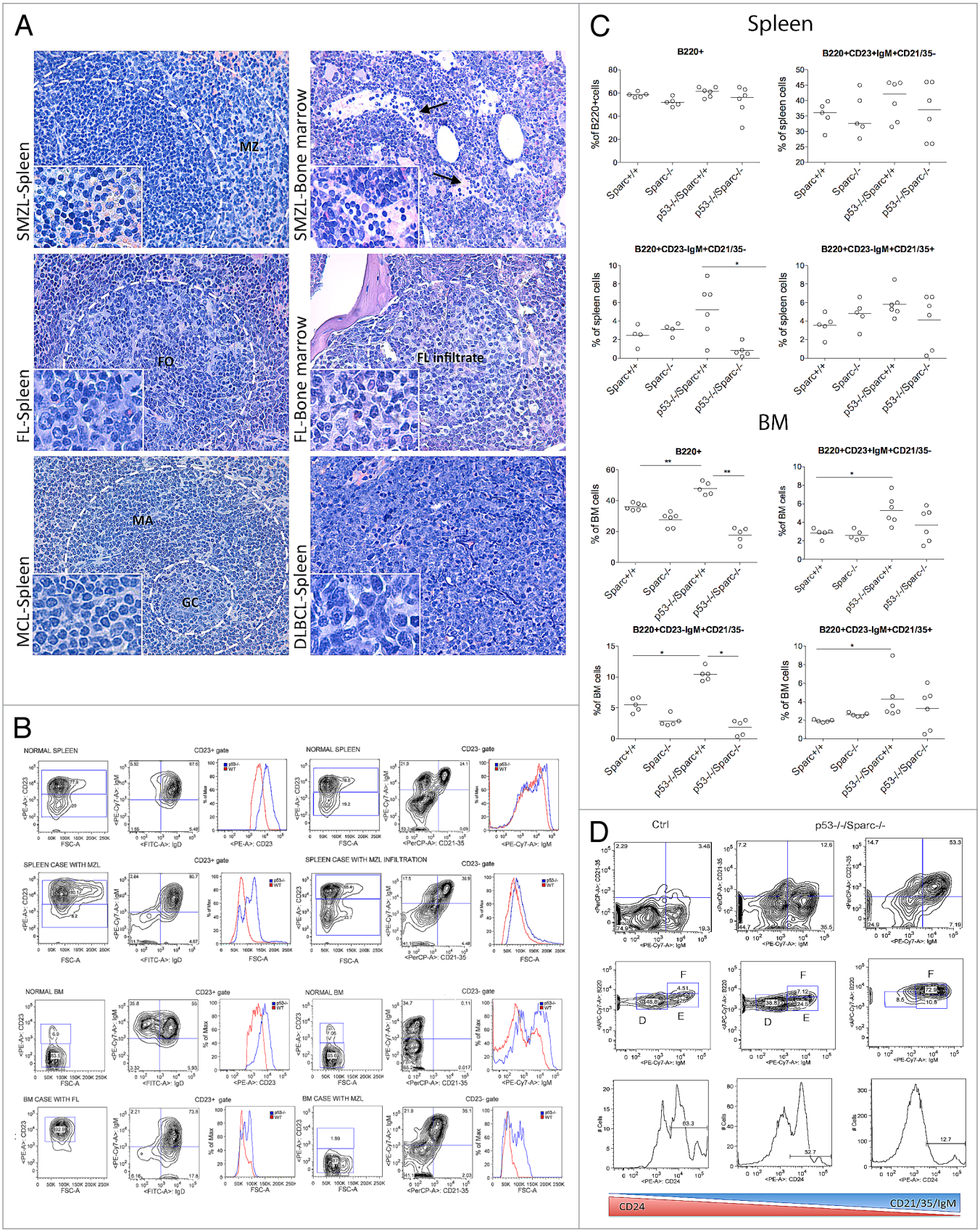

Figure 9. For figure legend, see page 15.

P-selectin ligands PSGL-1 and CD24.[31,32] These molecules are intimately involved in the immune cell trafficking to hematopoietic tissues.[33] Furthermore, their expression on malignant hematopoietic cells is well known and correlates with neoplastic cells homing within different hematopoietic stromal niches.[26,34,35] As far as CD24 is concerned, a specific function in the normal and malignant lymphopoietic homeostasis has not been defined yet. CD24 neutralizes the function of the chemokine (C-X-C) motif receptor 4 (CXCR4) expressed in pre-B cells and human breast cancer cells.[36] CXCR4 retains B cell precursors in close contact with CXCL12-expressing stromal cells in the hematopoietic environment, a mechanism that is also active in some B-cell neoplasms such as CLL.[37] Thus, the CXCR4/CD24/P-selectin axis might be functionally relevant for the homing/survival of lymphoma cells within the BM niche. Indeed, the lack of CD24 in pre-B acute lymphoblastic leukemia has been associated with radiation resistance of primary clonogenic blasts.[38] Consistently, in our experiments in vivo, we found that the lymphoid populations that were expanded in *p53*$^{-/-}$ and *p53*$^{-/-}$/*Sparc*$^{-/-}$ mice with splenic lymphomas, showed a decrease in CD24 expression when infiltrating the BM, which was more prominent in the *p53*$^{-/-}$/*Sparc*$^{-/-}$ setting constintently with the enhanced micro-environmental expression of the ligand P-selectin. Through the modulation of adhesive properties of the BM stromal microenvironment, SPARC could not only affect the fitness of B-cell precursors but also influence the BM infiltration by splenic lymphomatous cells.

Another important aspect of the SPARC-mediated regulation of the BM niche is its reversible nature, as suggested by secondary BMT experiments in which *Sparc*$^{-/-}$ HSC "educated" into a WT recipient were rendered defective in their B-cell lymphopoietic function upon retransplantation into a *Sparc*$^{-/-}$ but not a WT recipient. This finding implies that variations in the quality of the ECM milieu can induce the loss or decrease of specific hematopoietic functions in the absence of HSC intrinsic defects.

In SPARC deficient mice, defective BM B-cell precursors lymphopoiesis due to faulty stromal composition of the niche finds correlates with similar deficiencies in splenic lymphopoiesis. Indeed, we showed that SPARC stromal deficiency impoverished the CD93^{+} T1 immature B-cell fraction, underscoring that the dependency of immature B-cell subsets from the integrity of stromal niches is extended to SLO. The stromal environments that, within SLO, harbor immature lymphoid cells are far less well characterized than those in the BM. We showed that splenic T1 B-cells reside in collagen-IV rich areas at the edge of the highly vascularized red pulp, a front-line in BM-SLO trafficking. These same areas were altered in their collagen architecture when SPARC was defective becoming more permissive to infiltration by non-lymphoid elements. The infiltration of SLO lymphoid niches by myeloid cells is emerging as a relevant event in the loss of lymphopoietic homeostasis.[10] Myeloid elements comprising granulocytes, macrophages and mast cells can dramatically change the quality of signals that lymphoid cells perceive within stromal niches by directly influencing the cytokine/chemokine milieu, (e.g., through IL-21, BlyS/Baff, IL-6, IL-10, etc.), providing activation signals to lymphoid cells through co-stimulatory ligands (e.g., CD40L, and CD80). Alternatively, these effects may also be mediated indirectly, by changing the activation status of mesenchymal cells. Notably, the magnitude and relevance of these changes are strictly dependent on the integrity of the ECM because a defective mesenchymal milieu not only determines the occurrence of unrestrained myeloid-lymphoid interactions but also depresses inhibitory signals from ECM receptors.[10] Functionally immature lymphoid cells are particularly sensitive to variations in the balance of signals inducing proliferative or differentiative outcomes. Within SLO, microenvironments populated by mature, yet plastic lymphoid cells and characterized by complex and dynamic equilibrium between apparently opposing pressures can be identified within the follicles. We showed here that the absence of SPARC affected the rate of spontaneous follicular and marginal lymphomagenesis in the *p53* mutant background. It is generally accepted that the understanding of normal B-cell development and the germinal center response is essential to comprehend the mechanisms governing GC-related B-cell lymphomas.[39] Indeed, pathways that are used by stroma-dependent clones, mostly during the early stages of lymphomagenesis, are very similar to those used during early B-cell development in the BM and during Ag-triggered B-cell expansion in follicle GC. The absence of SPARC has been observed to affect GC responses in vivo[9] but also to decrease the frequency of FL occurrence in the spleen of *p53*$^{-/-}$ mice, suggesting that similarly to immature B-cell niches, the GC mesenchymal environment may also lose important signals to regulate normal and transforming B-cells, owing to the defective ECM composition. Importantly, these same defects may impact advanced steps in FL progression, such as the colonization of the BM osteoblastic niche, which is characterized by SPARC upregulation.

A different influence was cast by SPARC deficiency on MZB cells and on their malignant transformation in *p53*$^{-/-}$ mice. Indeed, in the *Sparc*$^{-/-}$ setting, all of the bystander mechanisms that have been described to sustain MZB differentiation and responses were enhanced, like the increased presence of

Figure 9. *p53*$^{-/-}$ spontaneous SLO lymphomagenesis and BM infiltration of malignant clones are hampered by Sparc deficiency. (**A**) Spleen and bone marrow (BM) histopathology showing prototypical cases of splenic marginal zone lymphoma (MZL), follicular lymphoma (FL), mantle cell lymphoma (MCL) and diffuse large B cell lymphoma, not otherwise specified (DLBCL/NOS) arising in *p53*$^{-/-}$ mice. The different BM infiltration patterns are consistent with the primary clone histotype, being for example nodular and para-trabecular in FL cases and prominently intrasinusoidal in SMZL. (**B**) Representative flow cytometry analyses showing the expansion of B220^{+}CD23^{+}IgM^{+}IgD^{+}CD21/35^{-} or B220^{+}CD23^{-}IgM^{-}IgD^{-}CD21/35^{+} B cells in *p53*$^{-/-}$ cases histopathologically diagnosed for FL or MZL. In *p53*$^{-/-}$ mouse BM and splenic preparations, the expanded lymphocyte population could also be distinguished by increased FSC, CD23 and IgM in comparison to their WT counterpart. (**C**) Collective data from cytofluorimetric analysis showing the enrichment in B-cell populations with B220^{+}CD23^{+}IgM^{+} CD21/35^{-} (follicular), B220^{+}CD23^{-}IgM^{+}CD21/35^{+} (marginal), and B220^{+}CD23^{-}IgM^{+}CD21/35^{-} (mantle/peripheral NOS) phenotype in the spleen and BM of *Sparc*$^{+/+}$ and *Sparc*$^{-/-}$ mice either *p53*$^{-/-}$ or *p53*$^{+/+}$ (n = 5 mice/group; one representative experiment out of 3). (**D**) Representative contour plots from flow cytometry analysis of a *p53*$^{-/-}$/*Sparc*$^{-/-}$ case with BM-infiltration by B220^{+}CD23^{-}IgM^{+}CD21/35^{+} MZL. These cells localize in the fraction F of the BM and are characterized by reduced CD24 expression in comparison to normal B cells localizing within the same fraction.

Table 1. Characterization of lymphomas arising in secondary lymphoid organs of p53 null mice either SPARC deficient or not and of their possible BM infiltration

			Flow cytometry of expanding cells							
Mouse #	**Sparc genotype**	**Histopathology (SLO = spleen)**	**B220+**	**CD23**	**CD21/35**	**IgD**	**IgM**	**FSC**	**BM infiltration**	**Localization of BM infiltration**
569	WT	high grade FL	pos	pos	neg	pos	pos	increased	yes	paratrabecular/ interstitial
497	WT	SMZL	pos	pos	dull/pos	nd	pos	increased	yes (10%)	interstitial, pervivascular
483	WT	FL and MZ hyperplasia	n/a	n/a	n/a	n/a	n/a	normal	absent	absent
496	WT	MCL	pos	neg	neg	nd	pos	increased		
8358	WT	DLBL	pos	pos	neg	pos	pos	increased	yes	nd
89	WT	high grade FL	pos	pos	dull	nd	pos	increased	yes	nd
40	WT	Early FL	pos	pos	dull/neg	pos	pos	increased	yes	nd
657	KO	FL	pos	high	dull/neg	pos	pos	increased	absent	absent
302	KO	Early FL	pos	pos	dull/neg	pos	pos	normal	absent	absent
306	KO	SMZL	pos	neg	pos	neg	pos	increased	yes (10%)	nd
179	KO	Normal architecture	n/a	n/a	n/a	n/a	n/a	n/a	absent	absent
33	KO	Normal architecture	n/a	n/a	n/a	n/a	n/a	n/a	absent	absent
10	KO	Normal architecture	n/a	n/a	n/a	n/a	n/a	n/a	absent	absent
20	KO	Normal architecture	n/a	n/a	n/a	n/a	n/a	n/a	absent	absent

Staining intensity: negative, mean of fluorescence (MFI) less than 10^2; dull, MFI between 10^2 and 10^3; positive: MFI between 10^3 and 10^4; bright, MFI up to 10^4; n/a: not applicable, the different lymphoid populations are normally represented; n/d: bone marrow evaluated only through flow cytometry.

B-helper neutrophils[20] or the increased production of DLL-1 and NOTCH engagement.[4] However, such conditions did not magnify MZB responses to NPP-Ficoll vaccination or increase the absolute incidence of SMZL in *p53*$^{-/-}$/*Sparc*$^{-/-}$ mice. A possible explanation for this picture stems from our recently reported mechanism of SMZL progression in human and in *p53*$^{-/-}$ mice. In both human and mouse, we showed the existence of a productive interaction between mesenchymal stromal cells and mast cells, via the CD40/CD40L axis, toward the production of a TNF- and IL-6-rich milieu sustaining MZB clones. Likely the absence of SPARC could affect this cross-talk in favor of other type of interactions. For example, granulocytes, which are overproduced in a stromal SPARC defective environment, may compete with mesenchymal cells for the interaction with mast cells. Accordingly, in *Sparc*-null mice neutrophils have been reported to overexpress CD40 in comparison to their WT counterparts.[10]

In conclusion, we have unveiled new immunoregulatory functions for the matricellular protein SPARC that warrant further investigations of this class of molecules in the physiology and pathogenesis of B-cell lymphomas.

Materials and Methods

Animals

BALB/cAnNCrl mice at 8–10 wk of age were purchased from Charles River Laboratories. CNCr.129S(B6)–*Sparc*^{tm1Hwe} mice were developed in our institute by crossing B6;129-*Sparc*^{tm1Hwe} mice (provided by Dr. Chin Howe; Wistar Institute) with BALB/cAnNCrl mice for 12 generations prior to intercrossing.[40] BALB/cJ-Trp53^{tm1Tyj} mice were kindly provided by Dr. Pier Luigi Lollini (University of Bologna). These mice were crossed with BALB/cAnNCrl mice and CNCr.129S(B6)–*Sparc*^{tm1Hwe} mice, and then intercrossed. CNCr-Trp53$^{tm1\ Tyj}$ mice and CNCr-Trp53^{tm1Ty} Sparc^{tm1Hwe} mice (referred to as *p53*$^{-/-}$/*Sparc*$^{+/+}$ and *p53*$^{-/-}$/*Sparc*$^{-/-}$ mice) and control wild-type (WT) mice were maintained in pathogen-free conditions in our animal facility. The *Trp53 g*enotype was distinguished by PCR analysis. These mice were bred and maintained at the Istituto Nazionale Tumori under standard conditions, according to institutional guidelines. Chimeric *Sparc*$^{-/-}$ > WT (Thy-1^b > Thy-1^a), WT > *Sparc*$^{-/-}$ (Thy-1^a > Thy-1^b), WT > WT(Thy-1^a > Thy-1^b), *Sparc*$^{-/-}$ > *Sparc*$^{-/-}$ (Thy-1^b > Thy-1^b) mice were obtained by BM transplantation as previously reported.[17] Engraftment was verified 6–8 wk after BM transplantation by immunocytometric analysis of peripheral

blood mononuclear cells according to Thy-1[a] (BD Biosciences) and Thy-1[b] (BD Biosciences) expression. The Institute Ethical Committee for animal use authorized these experiments.

Lymphoma patient histopathology and immunohistochemistry

For the analyses on human specimens, 197 cases of B-cell non-Hodgkin lymphoma patient tissue specimens, consecutively diagnosed between 2004 and 2013, were collected from the archives of the Human Pathology Section of the Department of Health Sciences, University of Palermo. Only cases with concomitant SLO and BM involvement were included. Moreover, 8 SLO samples with follicular hyperplasia (5 lymph nodes and 3 tonsils), 3 normal spleen parenchyma samples, 5 normal BM samples and 3 BM samples with signs of trabecular bone remodeling (2 primary myelofibrosis samples and one reactive sample) were selected. IHC was performed as previously described[8] using the streptavidin-biotin-peroxidase complex method with the following primary antibodies (Abs): anti-human SPARC (clone ON1–1, Takara); anti-human CD146 (clone N1238, Novocastra); anti-human fibronectin (clone F1, AbCam); anti-human collagen I (I-8H5, Acris Antibodies, Germany), anti-human CD271 (clone 7F10, Novocastra), anti-human CD20 (clone L26, Novocastra), anti-human CXCL-12 (clone 79018, R&D System), anti-human Jagged-1 (clone EPR4290, Epitomics), anti-human CD62P (clone C34, Novocastra). Aminoethyl-carbazole (AEC; (Dako Cytomation) was used as the chromogenic substrate. Negative control staining was performed using mouse, rabbit or goat immune sera instead of the primary Abs. In double-marker IHC stainings, tissue samples were incubated, by sequential immunostaining, with primary antibodies against SPARC (clone ON1–1, Takara), revealed using LSAB + AP and 5-Bromo-4-chloro-3-indolyl phosphate (BCIP)/nitro blue tetrazolium chloride (NBT; DAKO) as chromogen, and either IgM (clone 8H6, Novocastra) or CD10 (clone56C6, Novocastra) detected by LSAB + HRP and AEC (DAKO) as chromogen. The same steps described above were used in double-marker immunofluorescence (IF) analyses on human tissues in which SPARC (clone ON1–1, Takara) and CD10 (clone56C6, Novocastra) or collagen type-I (I-8H5, Acris Antibodies) were revealed by either Alexa-488 or Alexa-568-conjugated specific secondary antibodies.

Confocal microscopy

The following primary monoclonal Abs (mAb) were used for triple IF staining on mouse tissues: APC- rat anti-mouse GR-1 (e-Biosciences); Alexa-546-conjugated rat anti-mouse IgM (Invitrogen); FITC-conjugated CD93: rat anti-mouse CD169 (e-Biosciences); goat anti-mouse SPARC/osteonectin (AF952, R&D System). In addition, polyclonal Abs against collagen type I and collagen type IV were used (Chemicon). Triple IF involving primary Ab not directly conjugated were performed through sequential steps as previously described.[10] Sections were analyzed with a Microradiance 2000 (Bio-Rad Laboratories) confocal microscope equipped with Ar (488 nm), HeNe (543 nm) and red laser diode (638 nm) lasers. Confocal images (512 × 512 pixels) were obtained using a 20 × , 0.5 NA Plan Fluor DIC or 60 × , 1.4 NA oil immersion lens and analyzed using ImagePro 7.0.1 software. Immersion oil (ISO 8036) was purchased from Merck.

Cytofluorimetric analysis

Six-color fluorescence cytometry was used to analyze the composition of the B-cell compartment in the BM and SLO, as previously described.[41] B-cell development in the BM has been classified into sequential subsets designated Fractions A, B, C, C', D, E, F by Hardy and colleagues. For BM analysis the following fluorophore-conjugated rat anti-mouse mAb were used: APC-eFluor 780-conjugated B220; APC-conjugated CD43; PECy7-conjugated- IgM; PE-conjugated CD24; FITC-conjugated BP-1. To assess apoptosis BM cell suspensions were stained with e-Fluor 710-conjugated annexin V according to the manufacturer's instructions. Splenic B-cell composition was analyzed, as previously described,[42] using the following rat anti-mouse mAb: APC-eFluor 780-conjugated B220; APC-conjugated CD93; PECy7-conjugated- IgM; PE-conjugated CD23; FITC-conjugated IgD and PerCP-conjugated CD21/35. LAIR-1 expression on immature cells was evaluated by using a rat anti mouse LAIR-1 PE-conjugated in combination with the APC-eFluor 780-conjugated B220, APC-conjugated CD93 or APC-conjugated CD43. Dll-1 expression in myeloid cells was evaluated by using the rat anti-mouse Dll-1 mAb. All Abs used for cytofluorimetric analysis were from e-Biosciences. Stained samples were run on a NAME flow cytometer, with NUMBER events acquired per sample. Analyses were performed using NAME software.

RNA extraction and qRT-PCR

B cells from the spleen of wt or Sparc−/− mice were purified using anti-CD19 microbeads (Miltenyi Biotech) according to manufacturer's instruction and resuspended in TRIzol (Invitrogen). RNA was purified by phenol/chloroform extraction followed by loading onto RNeasy MINI kit (Qiagen). On-column DNase treatment was routinely performed. RNA purity and yield was assessed using NanoDrop. RNA was reverse transcribed using High Capacity cDNA Reverse Transcription Kit (Applied Biosystems). qPCR reaction was prepared using TaqMan® Fast Universal PCR Master Mix and run on a 7900HT Fast Real-Time PCR system (Applied Biosystems). The following TaqMan® probes were used: Gapdh (Mm03302249_g1) and Dtx1 (Mm00492297_m1).

Gene profile analysis

Normalized gene expression data from Greenbaum et al.[1] were downloaded from NCBI's Gene Expression Omnibus (www.ncbi.nlm.nih.gov/geo; accession, GSE43613). *Sparc* expression was evaluated in comparison with known mesenchymal-expressed genes (*Itgb1*, *Lgals1*, *Pdgfra*) in CXCL12$^+$ reticular cells (2 replicate samples) and PDGFRα$^+$ Sca$^+$ stromal cells.

Disclosure of Potential Conflicts of Interest

No potential conflicts of interest were disclosed.

Grant Support

This work was supported by the Association for International Cancer Research (AICR UK, grant n° 11–0595) and the Associazione Italiana per la Ricerca sul Cancro (Investigator Grants n° 10137 to M.P.C.; My First Grant n° 12810 to S.S. and Program Innovative Tools for Cancer Risk Assesment and Diagnosis, 5 per mille grant number 12162 to M.P.C. and C.T.).

References

1. Greenbaum A, Hsu YM, Day RB, Schuettpelz LG, Christopher MJ, Borgerding JN, Nagasawa T, Link DC. CXCL12 in early mesenchymal progenitors is required for haematopoietic stem-cell maintenance. Nature 2013; 495:227-30; PMID:23434756; http://dx.doi.org/10.1038/nature11926
2. Egawa T, Kawabata K, Kawamoto H, Amada K, Okamoto R, Fujii N, Kishimoto T, Katsura Y, Nagasawa T. The earliest stages of B cell development require a chemokine stromal cell-derived factor/pre-B cell growth-stimulating factor. Immunity 2001; 15:323-34; PMID:11520466; http://dx.doi.org/10.1016/S1074-7613(01)00185-6
3. Sudo T, Ito M, Ogawa Y, Iizuka M, Kodama H, Kunisada T, Hayashi S, Ogawa M, Sakai K, Nishikawa S. Interleukin 7 production and function in stromal cell-dependent B cell development. J Exp Med 1989; 170:333-8; PMID:2787384; http://dx.doi.org/10.1084/jem.170.1.333
4. Pillai S, Cariappa A. The follicular versus marginal zone B lymphocyte cell fate decision. Nat Rev Immunol 2009; 9:767-77; PMID:19855403; http://dx.doi.org/10.1038/nri2656
5. Treanor B, Depoil D, Gonzalez-Granja A, Barral P, Weber M, Dushek O, Bruckbauer A, Batista FD. The membrane skeleton controls diffusion dynamics and signaling through the B cell receptor. Immunity 2010; 32:187-99; PMID:20171124; http://dx.doi.org/10.1016/j.immuni.2009.12.005
6. Song J, Lokmic Z, Lämmermann T, Rolf J, Wu C, Zhang X, Hallmann R, Hannocks MJ, Horn N, Ruegg MA, et al. Extracellular matrix of secondary lymphoid organs impacts on B-cell fate and survival. Proc Natl Acad Sci U S A 2013; 110:E2915-24; PMID:23847204; http://dx.doi.org/10.1073/pnas.1218131110
7. Lu P, Weaver VM, Werb Z. The extracellular matrix: a dynamic niche in cancer progression. J Cell Biol 2012; 196:395-406; PMID:22351925; http://dx.doi.org/10.1083/jcb.201102147
8. Tripodo C, Sangaletti S, Guarnotta C, Piccaluga PP, Cacciatore M, Giuliano M, Franco G, Chiodoni C, Sciandra M, Miotti S, et al. Stromal SPARC contributes to the detrimental fibrotic changes associated with myeloproliferation whereas its deficiency favors myeloid cell expansion. Blood 2012; 120:3541-54; PMID:22955913; http://dx.doi.org/10.1182/blood-2011-12-398537
9. Piconese S, Costanza M, Tripodo C, Sangaletti S, Musio S, Pittoni P, Poliani PL, Burocchi A, Passafaro AL, Gorzanelli A, et al. The matricellular protein SPARC supports follicular dendritic cell networking toward Th17 responses. J Autoimmun 2011; 37:300-10; PMID:21962567; http://dx.doi.org/10.1016/j.jaut.2011.09.002
10. Sangaletti S, Tripodo C, Vitali C, Portararo P, Guarnotta C, Casalini P, Cappetti B, Miotti S, Pinciroli P, Fuligni F, et al. Defective stromal remodeling and neutrophil extracellular traps in lymphoid tissues favor the transition from autoimmunity to lymphoma. Cancer Discov 2014; 4:110-29; PMID:24189145; http://dx.doi.org/10.1158/2159-8290.CD-13-0276
11. Hardy RR, Hayakawa K. B cell development pathways. Annu Rev Immunol 2001; 19:595-621; PMID:11244048; http://dx.doi.org/10.1146/annurev.immunol.19.1.595
12. Suzuki T, Kiyokawa N, Taguchi T, Sekino T, Katagiri YU, Fujimoto J. CD24 induces apoptosis in human B cells via the glycolipid-enriched membrane domains/rafts-mediated signaling system. J Immunol 2001; 166:5567-77; PMID:11313396; http://dx.doi.org/10.4049/jimmunol.166.9.5567
13. Carsetti R. The development of B cells in the bone marrow is controlled by the balance between cell-autonomous mechanisms and signals from the microenvironment. J Exp Med 2000; 191:5-8; PMID:10620600; http://dx.doi.org/10.1084/jem.191.1.5
14. Taguchi T, Kiyokawa N, Mimori K, Suzuki T, Sekino T, Nakajima H, Saito M, Katagiri YU, Matsuo N, Matsuo Y, et al. Pre-B cell antigen receptor-mediated signal inhibits CD24-induced apoptosis in human pre-B cells. J Immunol 2003; 170:252-60; PMID:12496407; http://dx.doi.org/10.4049/jimmunol.170.1.252
15. Aigner S, Sthoeger ZM, Fogel M, Weber E, Zarn J, Ruppert M, Zeller Y, Vestweber D, Stahel R, Sammar M, et al. CD24, a mucin-type glycoprotein, is a ligand for P-selectin on human tumor cells. Blood 1997; 89:3385-95; PMID:9129046
16. Lebbink RJ, de Ruiter T, Verbrugge A, Bril WS, Meyaard L. The mouse homologue of the leukocyte-associated Ig-like receptor-1 is an inhibitory receptor that recruits Src homology region 2-containing protein tyrosine phosphatase (SHP)-2, but not SHP-1. J Immunol 2004; 172:5535-43; PMID:15100296; http://dx.doi.org/10.4049/jimmunol.172.9.5535
17. Sangaletti S, Tripodo C, Cappetti B, Casalini P, Chiodoni C, Piconese S, Santangelo A, Parenza M, Arioli I, Miotti S, et al. SPARC oppositely regulates inflammation and fibrosis in bleomycin-induced lung damage. Am J Pathol 2011; 179:3000-10; PMID:22001347; http://dx.doi.org/10.1016/j.ajpath.2011.08.027
18. McKearn JP, Baum C, Davie JM. Cell surface antigens expressed by subsets of pre-B cells and B cells. J Immunol 1984; 132:332-9; PMID:6606670
19. Chiodoni C, Colombo MP, Sangaletti S. Matricellular proteins: from homeostasis to inflammation, cancer, and metastasis. Cancer Metastasis Rev 2010; 29:295-307; PMID:20386958; http://dx.doi.org/10.1007/s10555-010-9221-8
20. Puga I, Cols M, Barra CM, He B, Cassis L, Gentile M, Comerma L, Chorny A, Shan M, Xu W, et al. B cell-helper neutrophils stimulate the diversification and production of immunoglobulin in the marginal zone of the spleen. Nat Immunol 2012; 13:170-80; PMID:22197976; http://dx.doi.org/10.1038/ni.2194
21. Morse HC 3rd, Anver MR, Fredrickson TN, Haines DC, Harris AW, Harris NL, Jaffe ES, Kogan SC, MacLennan IC, Pattengale PK, et al.; Hematopathology subcommittee of the Mouse Models of Human Cancers Consortium. Bethesda proposals for classification of lymphoid neoplasms in mice. Blood 2002; 100:246-58; PMID:12070034; http://dx.doi.org/10.1182/blood.V100.1.246
22. Fredrickson TN, Lennert K, Chattopadhyay SK, Morse HC 3rd, Hartley JW. Splenic marginal zone lymphomas of mice. Am J Pathol 1999; 154:805-12; PMID:10079258; http://dx.doi.org/10.1016/S0002-9440(10)65327-8
23. Franco G, Guarnotta C, Frossi B, Piccaluga PP, Boveri E, Gulino A, Fuligni F, Rigoni A, Porcasi R, Buffa S, et al. Bone marrow stroma CD40 expression correlates with inflammatory mast cell infiltration and disease progression in splenic marginal zone lymphoma. Blood 2014; 123:1836-49; PMID:24452203; http://dx.doi.org/10.1182/blood-2013-04-497271
24. Sangaletti S, Di Carlo E, Gariboldi S, Miotti S, Cappetti B, Parenza M, Rumio C, Brekken RA, Chiodoni C, Colombo MP. Macrophage-derived SPARC bridges tumor cell-extracellular matrix interactions toward metastasis. Cancer Res 2008; 68:9050-9; PMID:18974151; http://dx.doi.org/10.1158/0008-5472.CAN-08-1327
25. Meyaard L. The inhibitory collagen receptor LAIR-1 (CD305). J Leukoc Biol 2008; 83:799-803; PMID:18063695; http://dx.doi.org/10.1189/jlb.0907609
26. Tripodo C, Sangaletti S, Piccaluga PP, Prakash S, Franco G, Borrello I, Orazi A, Colombo MP, Pileri SA. The bone marrow stroma in hematological neoplasms--a guilty bystander. Nat Rev Clin Oncol 2011; 8:456-66; PMID:21448151; http://dx.doi.org/10.1038/nrclinonc.2011.31
27. Piccaluga PP, De Falco G, Kustagi M, Gazzola A, Agostinelli C, Tripodo C, Leucci E, Onnis A, Astolfi A, Sapienza MR, et al. Gene expression analysis uncovers similarity and differences among Burkitt lymphoma subtypes. Blood 2011; 117:3596-608; PMID:21245480; http://dx.doi.org/10.1182/blood-2010-08-301556
28. Haylock DN, Nilsson SK. Osteopontin: a bridge between bone and blood. Br J Haematol 2006; 134:467-74; PMID:16848793; http://dx.doi.org/10.1111/j.1365-2141.2006.06218.x
29. Grassinger J, Haylock DN, Storan MJ, Haines GO, Williams B, Whitty GA, Vinson AR, Be CL, Li S, Sørensen ES, et al. Thrombin-cleaved osteopontin regulates hemopoietic stem and progenitor cell functions through interactions with alpha9beta1 and alpha4beta1 integrins. Blood 2009; 114:49-59; PMID:19417209; http://dx.doi.org/10.1182/blood-2009-01-197988
30. Boyerinas B, Zafrir M, Yesilkanal AE, Price TT, Hyjek EM, Sipkins DA. Adhesion to osteopontin in the bone marrow niche regulates lymphoblastic leukemia cell dormancy. Blood 2013; 121:4821-31; PMID:23589674; http://dx.doi.org/10.1182/blood-2012-12-475483
31. Tripodo C, Florena AM, Macor P, Di Bernardo A, Porcasi R, Guarnotta C, Ingrao S, Zerilli M, Secco E, Todaro M, et al. P-selectin glycoprotein ligand-1 as a potential target for humoral immunotherapy of multiple myeloma. Curr Cancer Drug Targets 2009; 9:617-25; PMID:19508173; http://dx.doi.org/10.2174/156800909789056971
32. Parlato M, Souza-Fonseca-Guimaraes F, Philippart F, Misset B, Adib-Conquy M, Cavaillon JM, Jacqmin S, Journois D, Lagrange A, Pinot de Villechenon G, et al.; Captain Study Group. CD24-triggered caspase-dependent apoptosis via mitochondrial membrane depolarization and reactive oxygen species production of human neutrophils is impaired in sepsis. J Immunol 2014; 192:2449-59; PMID:24501201; http://dx.doi.org/10.4049/jimmunol.1301055
33. Vermeulen M, Le Pesteur F, Gagnerault MC, Mary JY, Sainteny F, Lepault F. Role of adhesion molecules in the homing and mobilization of murine hematopoietic stem and progenitor cells. Blood 1998; 92:894-900; PMID:9680357
34. Tripodo C, Florena AM, Porcasi R, Ingrao S, Guarnotta C, Franco V. Constant detection of cyclooxygenase 2 in terminal stages of myeloid maturation. Acta Haematol 2007; 117:48-50; PMID:17095859; http://dx.doi.org/10.1159/000096788
35. Cacciatore M, Guarnotta C, Calvaruso M, Sangaletti S, Florena AM, Franco V, Colombo MP, Tripodo C. Microenvironment-centred dynamics in aggressive B-cell lymphomas. Adv Hematol 2012; 2012:138079; PMID:22400028; http://dx.doi.org/10.1155/2012/138079
36. Schabath H, Runz S, Joumaa S, Altevogt P. CD24 affects CXCR4 function in pre-B lymphocytes and breast carcinoma cells. J Cell Sci 2006; 119:314-25; PMID:16390867; http://dx.doi.org/10.1242/jcs.02741
37. Burger JA, Burger M, Kipps TJ. Chronic lymphocytic leukemia B cells express functional CXCR4 chemokine receptors that mediate spontaneous migration beneath bone marrow stromal cells. Blood 1999; 94:3658-67; PMID:10572077
38. Uckun FM, Song CW. Lack of CD24 antigen expression in B-lineage acute lymphoblastic leukemia is associated with intrinsic radiation resistance of primary clonogenic blasts. Blood 1993; 81:1323-32; PMID:8443393

39. Natkunam Y. The biology of the germinal center. Hematology Am Soc Hematol Educ Program 2007; 210-5; PMID:18024632; http://dx.doi.org/10.1182/asheducation-2007.1.210
40. Sangaletti S, Stoppacciaro A, Guiducci C, Torrisi MR, Colombo MP. Leukocyte, rather than tumor-produced SPARC, determines stroma and collagen type IV deposition in mammary carcinoma. J Exp Med 2003; 198:1475-85; PMID:14610043; http://dx.doi.org/10.1084/jem.20030202
41. Tung JW, Parks DR, Moore WA, Herzenberg LA, Herzenberg LA. Identification of B-cell subsets: an exposition of 11-color (Hi-D) FACS methods. Methods Mol Biol 2004; 271:37-58; PMID:15146111
42. Kanayama N, Cascalho M, Ohmori H. Analysis of marginal zone B cell development in the mouse with limited B cell diversity: role of the antigen receptor signals in the recruitment of B cells to the marginal zone. J Immunol 2005; 174:1438-45; PMID:15661902; http://dx.doi.org/10.4049/jimmunol.174.3.1438